Effective interactions in liquid ^{3}He

H. R. Glyde
Department of Physics, University of Delaware, Newark, Delaware 19711

S. I. Hernadi
Department of Physics, University of Ottawa, Ottawa, Ontario, Canada K1N 6N5
(Received 22 November 1982; revised manuscript received 6 April 1983)

The effective interaction between a pair of ^{3}He atoms in liquid ^{3}He is calculated within the Galitskii-Feynman (GF) T-matrix approximation. With the use of this T matrix, the single-particle energy spectrum $\epsilon(k)$ is calculated in the Hartree-Fock (HF) limit. This continuous $\epsilon(k)$ is used as an input spectrum for the T matrix (for both initial and intermediate states), and $\epsilon(k)$ and the T matrix Γ are evaluated iteratively until consistent. We believe this is the first fully iterative calculation using a continuous $\epsilon(k)$ in ^{3}He. We find (a) that the total $E\approx -3.7$ K at the observed saturated-vapor-pressure volume is much lower than values ($E\approx -1.0$ K) found previously with the use of a spectrum having a gap at the Fermi surface $k=k_F$, (b) that any continuous $\epsilon(k)$ in Γ leads generally to a much lower E [and $\epsilon(k)$] than one having a gap at k_F, (c) that the scattering to intermediate hole states included in the GF T matrix does not change Γ, $\epsilon(k)$, or E significantly from the more usual Brueckner-Bethe-Goldstone T matrix for which only scattering to intermediate particle states is allowed, (d) that the rearrangement contributions to $\epsilon(k)$ are negligible with the use of the GF T matrix making the dynamical and statistical $\epsilon(k)$ the same in the T-matrix approximation, (e) that in the HF approximation, $m^*(k)\approx 0.9$ largely independent of k, and (f) that, when the energy dependence of the self-energy is included, $m^*(k,E)$ is enhanced at $k\approx k_F$ and somewhat above k_F, especially at smaller volumes.

I. INTRODUCTION

The discovery of superfluid phases,[1,2] the measurement of elementary excitations by neutron scattering,[3] the possibility[4] of highly polarized ^{3}He, and the recent controversy over the effective mass[5] have sparked a renewed interest[6–12] in the interaction between atoms in liquid ^{3}He. This paper is devoted to a microscopic study of this interaction.

In Landau's renowned theory[13,14] of Fermi liquids, the effective interaction between quasiparticles is parametrized. The values of the parameters are obtained from fits to experiment. His theory, the notion of quasiparticles, and the form of the interaction between them have all found a solid foundation in microscopic, many-body theory.[15] However, an explicit calculation of the effective interaction between quasiparticles from first principles has proved very complicated. Recent variational calculations[16] have been more successful in predicting the ground-state energy (finding $E\approx -2.2$ K compared with the observed $E=-2.5$ K). Some early studies of the effective interaction we have found particularly illuminating are the following: Abrikosov and Khalatnikov,[17] Hone,[18] Emery and Sessler,[19] Emery,[20] Burkhardt,[21] and more recently Babu and Brown.[22]

The pioneering work of Brueckner and Gammel[23] stands out as the first microscopic calculation of the properties of ^{3}He beginning with a realistic potential. They used Hartree-Fock (HF) theory coupled with a K-matrix treatment of the pair interaction.[24] They evaluated the K matrix and the single-particle energy (SPE) spectrum $\epsilon(k)$ self-consistently for wave vectors k up to the Fermi wave vector k_F. For $k>k_F$, they approximated the $\epsilon(k)$ by free-particle energies. The spectrum, therefore, had a gap at $k=k_F$, which excludes the possibilities of zeros in the energy denominator of the K matrix and ensures that K is real. The K matrix formulated using Rayleigh-Schrödinger perturbation theory by Brueckner[24] and by Bethe and Goldstone[25] implicitly requires a gap in $\epsilon(k)$ so that K is real. Brueckner and Gammel (BG) obtained semiquantitative results and a minimum total energy $E=-0.96$ K at a volume $\sim 25\%$ greater than the observed volume.

Østgaard,[26] in a series of careful papers, calculated many properties of ^{3}He using the BG K-matrix theory and a model (reference) input SPE spectrum. As in the Brueckner and Gammel calculation, this model spectrum had a gap at $k=k_F$ with the intermediate-state spectrum lying above the initial-state spectrum. He obtained, including three-body terms, a minimum total energy [Ref. 26(c)] $E=-1.0$ K at a volume $\sim 10\%$ greater than the observed volume. Particularly, including rearrangement terms, he obtained [Ref. 26(a)] reasonable values for the Landau parameters.

Bishop, Ghassib, Irvine, and Strayer[27–29] have made extensive calculations of the Galitskii-Feynman[30] (GF) T matrix using an input SPE spectrum approximated by free-particle energies. The GF T matrix differs from the Brueckner-Bethe-Goldstone (BBG) K matrix by including scattering to intermediate hole states as well as to intermediate particle states. Also, the GF, T matrix is derived using Green-function methods, and it is more natural to use a continuous SPE energy spectrum, such as free-particles energies, $\epsilon(k)=\hbar^2k^2/2m$, having no gap. Ghassib *et al.*[27] found an interesting singularity in the $L=0$ component of this T matrix at negative, off-shell energies.

Here we apply to ^{3}He a textbook HF theory coupled with the GF T matrix. A BBG-type approximation, in which scattering to particle states only is allowed, is also evaluated; but in each case a continuous SPE spectrum is used. The continuous HF single-particle energy spectrum is calculated self-consistently using the T matrix. Since the initial and intermediate states have the same $\epsilon(k)$, zeros occur in the energy denominator. The GF formulation includes an explicit path of integration around the zeros so that the resulting T matrix is always integrable and well defined, although complex.

A central aim here is to compare the effective interaction and SPE spectrum obtained using a continuous spectrum with those obtained by Brueckner and Gammel[23] and by Østgaard[26] using spectra having a gap. We find substantially increased binding for a continuous spectrum, largely independent of the form of the continuous spectrum. A second aim is to examine how the GF T matrix, calculated by Ghassib *et al.*,[27] changes when it and the SPE spectrum are calculated iteratively until consistent. Briefly, we find that the T matrix changes little, but that the SPE spectrum lies $\sim 12-15$ K below the free-particle spectrum. We also wish to compare the GF and BG T matrices. Using the GF T matrix we calculate several properties of liquid ^{3}He in the HF approximation.

The T matrix describes only part of the total effective interaction.[6,7,15,24] It takes account of the repeated scattering of a pair of ^{3}He atoms. This component of the pair interaction is dominated by the repulsive core of the bare interatomic pair potential and is often denoted the direct part of the interaction. Another purpose here is to examine how well the direct part represents the whole interaction. This we do by evaluating the Landau parameters and effective mass. Also at high-momentum transfers the direct part should dominate. A complete calculation of the T matrix for high-momentum transfers might represent the whole interaction well enough that it could be used in the calculation of the dynamic form factor $S(q,E)$ of liquid ^{3}He for comparison with neutron scattering measurements.[3]

In Secs. II and III we outline the HF T-matrix theory and discuss the equations actually evaluated here. In Sec. IV, we present T-matrix values obtained using model and free-particle input spectrum. The self-consistent SPE and T matrices are presented in Sec. V. The results are discussed in Sec. VI.

II. BACKGROUND THEORY

We begin with N ^{3}He atoms of mass M ($=3$ amu) in volume Ω (density $n=\Omega_0^{-1}=N/\Omega$). The Hamiltonian is

$$H=\sum_i \frac{p_i^2}{2M}+\sum_{\substack{i,j\\ i<j}} U_0(|x_i-x_j|)\,. \tag{1}$$

Here U_0 is a central, pairwise potential. Three-body and higher-order interactions are neglected and believed to be small. (They contribute[31] less than 2% to the ground-state energy of liquid ^{4}He, for example.) For U_0 we use the Beck[32] potential

$$U_0(x)=\epsilon\left[A'e^{-\alpha r-\beta r^6}-\frac{D}{(r^2+a^2)^3}\left[1+\frac{2.709+3a^2}{(r^2+a^2)}\right]\right],$$

with $\epsilon=10.371$ K, $A'=44.62\times10^4$, $\alpha=4.390$ Å^{-1}, $D=972.5$, $\beta=3.746\times10^{-4}$ Å^{-6}, and $a=0.675$ A. Since Østgaard[26] and Ghassib *et al.*[27] use the Yntema-Schneider[33] (YS) potential, we have used this potential in some specific comparisons with their results. We have also used the HFDHE2 potential of Aziz *et al.*[34] in one specific case to check the dependence of the effective interaction Γ on the potential. We find essentially no difference in Γ for the HFDHE2 and Beck potentials. The HFDHE2 potential is regarded as the most accurate available except possibly for the extreme short-range limit.[35]

In the HF theory we begin by ignoring U_0 entirely in H. Each particle then has a well-defined momentum p. To obtain the HF approximation we include the two terms (direct and exchange) that appear as first-order corrections for U_0 in the one-particle Green function G_1. To obtain the T-matrix approximation, we include, in addition, all those higher-order corrections to G_1 which correspond to interactions between pairs of ^{3}He atoms only. With this sum of repeated pair interaction terms, the HF form for G_1 is retained but U_0 is replaced by the Galitskii-Feynman effective interaction Γ yielding the Galitskii-Feynman-Hartree-Fock (GFHF) approximation. The GFHF approximation is derived in several texts but we refer specifically to Fetter and Walecka[36] where the equations we solve are derived explicitly.

The ground-state energy in the GFHF approximation[36] is

$$E=\sum_1 \frac{p_1^2}{2M}n(1)+\frac{1}{2\Omega}\sum_{1,2}[\Gamma(12;12)-\delta_{\sigma_1\sigma_2}\Gamma(21;12)]n(1)n(2)\,, \tag{2}$$

where

$$n(1)=(e^{\beta(\epsilon_1-\mu)}+1)^{-1}$$

is the Fermi function, $\beta=(k_BT)^{-1}$, and μ is the chemical potential. The sums 1 and 2 run over the free-particle momentum states and both spin states. $\Gamma(34;12)$ is the effective interaction (scattering amplitude) between a pair of otherwise free particles having initial momentum p_1 and p_2 before scattering and final momentum p_3 and p_4 after scattering:

$$\Gamma(34;12)=U_0(34;12)+\frac{1}{\Omega}\sum_{p_5,p_6}U_0(34;56)G_2^{\rm HF}(56;12)\Gamma(56;12)\,. \tag{3}$$

Here

$$G_2^{\rm HF}(56;12)=\left[\frac{(1-n_5)(1-n_6)}{E_{12}-\epsilon_5-\epsilon_6+i\eta}-\frac{n_5n_6}{E_{12}-\epsilon_5-\epsilon_6-i\eta}\right] \tag{4}$$

is the Fourier transform of the two-particle Green function in the HF approximation,

$$G_2^{\rm HF}(56,t)=-\frac{i}{\hbar}\langle Ta_5(t)a_6(t)a_6^\dagger(0)a_5^\dagger(0)\rangle_{\rm HF}\ .$$

The ϵ are the HF single-particle energies. For the on-energy-shell case needed in (2), E_{12} is set at the incoming energy of the interacting pair,

$$E_{12}=\epsilon_1+\epsilon_2\ . \tag{5}$$

In the Galitskii-Feynmann, Green-function formulation, the initial states before scattering [$\epsilon(p_1)$ and $\epsilon(p_2)$], the intermediate states [$\epsilon(p_5)$ and $\epsilon(p_6)$], and the final states after scattering [$\epsilon(p_3)$ and $\epsilon(p_4)$] of the interacting pair are all given by the same continuous spectrum $\epsilon(p)$. This differs, for example, from the Brueckner-Gammel calculation in which the initial- and intermediate-state spectra differ with a gap in the spectrum at P_F. Lejeune and Mahaux[37] argue that a continuous $\epsilon(p)$ is more consistent for determining single-particle properties [such as $\epsilon(p)$ and the effective mass] while Brandow[38] has compared the convergence of E in the two cases.

Once a continuous $\epsilon(p)$ is selected there remain many possible choices for its form. We define the SPE spectrum as

$$\epsilon(p_1,\sigma_1)=\frac{p_1^2}{2M}+\Sigma_1(1)+\Sigma_R(1)\ , \tag{6}$$

where

$$\Sigma_1(1)=\frac{1}{\Omega}\sum_{p_2,\sigma_2}[\Gamma(12;12)-\delta_{\sigma_1\sigma_2}\Gamma(21;12)]n(2) \tag{7}$$

and

$$\Sigma_R(1)=\frac{1}{2\Omega}\sum_{\substack{p_2,\sigma_2,\\ p_3,\sigma_3}}\left[\frac{\partial}{\partial n(1)}[\Gamma(32;32)-\delta_{\sigma_1\sigma_2}\Gamma(23;32)]\right]\times n(2)n(3)\ . \tag{8}$$

This SPE can be obtained as a functional derivative of the HF E, $\epsilon(1)\equiv\delta E/\delta n(1)$, and corresponds to Landau's definition[13,14] of ϵ. Here, however, we retain both the real and imaginary parts of Γ so Σ_1 is complex, which strictly lies outside the Landau definition. The present Σ_1 is also an approximation to the full self-energy Σ_1 appearing[36] in the HF single-particle Green function $G_1^{\rm HF}(p,\omega)$:

$$\Sigma_1(1,\omega_1)=\frac{-i}{\Omega}\sum_2\int\frac{d\omega_2}{2\pi}G_1^{\rm HF}(2,\omega_2)\times[\Gamma(12;12)-\delta_{\sigma_1\sigma_2}\Gamma(21;12)]\ . \tag{9}$$

In $\Sigma_1(1,\omega_1)$, the Γ depends on $E_{12}=\omega_1+\omega_2$ and is energy dependent. If we approximate Γ in (9) by its on energy-shell value ($\omega_1=\epsilon_1$, $\omega_2=\epsilon_2$) the integration over ω_2 in (9) leads directly to (7). The resulting $\Sigma_1(1,\epsilon_1)\equiv\Sigma_1(1)$ then depends only on momentum p_1. The Σ_R is called the rearrangement energy[39] and takes account of the rearrangement of state occupation in the fluid when a particle is removed (or added). It simulates to some extent the cooperative nature of the fluid and, therefore, strictly goes beyond the HF approximation. Since we hope eventually to use the present results in the long-wave limit, where collective effects are important, we felt it appropriate to include Σ_R at this stage. However, it is an arguable philosophical point whether Σ_R should be included. In any event, for the Galitskii-Feynman Γ where the full $G_2^{\rm HF}$ is retained, the Σ_R turns out to be numerically small.

Equations (3), (4), and (6) make up the GFHF approximation and clearly must be solved iteratively until consistent. The first term of $G_2^{\rm HF}$ in (4) corresponds to allowing scattering of the pair to intermediate particle states p_5 and p_6 generally above the Fermi momentum p_F. The second term in (4) is interpreted as scattering to intermediate hole states generally within the Fermi sea. In the Galitskii-Feynman (GF) case we retain the full $G_2^{\rm HF}$ (particle and hole states).

If we keep only the first term in $G_2^{\rm HF}$ (intermediate particle states only) we obtain the Brueckner-Bethe-Goldstone[24,25] (BBG) case. The present equations (2), (3), and (6) differ from the original BBG derivation only in the use of a continuous $\epsilon(k)$ and the resulting imaginary part to Γ.

III. TECHNICALITIES

A. Effective interaction

In this section we reduce Γ to the form evaluated. Firstly, since U_0 is a central, pairwise potential, its Fourier transform $U_0(34,12)$ depends only upon the momentum transfer $\hbar\vec{q}\equiv\vec{p}_3-\vec{p}_1$,

$$U_0(34,12)=U_0(3-1)\ .$$

Secondly, we assume the center of mass momentum, $\boldsymbol{P}$, is conserved in all scatterings,

$$\vec{P}=\vec{p}_1+\vec{p}_2=\vec{p}_5+\vec{p}_6=\vec{p}_3+\vec{p}_4\ .$$

The sums over $\vec{p}_5$ and $\vec{p}_6$ in (3) are therefore not independent, and

$$\Gamma(34;12)=U_0(3-1)+\frac{1}{\Omega}\sum_5 U_0(3-5)G_2^{\rm HF}(56;12)\Gamma(56;12)\ ,$$

with $6=\vec{P}-5$. We then introduce the initial relative momentum

$$\hbar\vec{k}=\vec{p}=\tfrac{1}{2}(\vec{p}_1-\vec{p}_2)\ ,$$

the final relative momentum

$$\hbar\vec{k}'=\vec{p}\,'=\tfrac{1}{2}(\vec{p}_3-\vec{p}_4)\ ,$$

and the intermediate relative momentum

$$\hbar\vec{k}_i=\vec{p}_i=\tfrac{1}{2}(\vec{p}_5-\vec{p}_6)\ ,$$

in terms of which $\vec{p}_3-\vec{p}_1=\vec{p}\,'-\vec{p}$ and $\vec{p}_3-\vec{p}_5=\vec{p}\,'-\vec{p}_i$, so that

$$\Gamma(\vec{p}\,';\vec{p},\vec{P})=U_0(\vec{p}\,'-\vec{p})+\frac{1}{\Omega}\sum_{p_i}U_0(\vec{p}\,'-\vec{p}_i)G_2^{\rm HF}(\vec{p}_i;\vec{p},\vec{P})\Gamma(\vec{p}_i;\vec{p},\vec{P})\ .$$

To evaluate Γ, we introduce an effective wave function in the momentum representation,

$$\chi(\vec{p}\,';\vec{p},\vec{P})=(2\pi)^3\delta(\vec{p}\,'-\vec{p})+G_2^{\rm HF}(\vec{p}\,';\vec{p},\vec{P})\frac{1}{\Omega}\sum_{p_i}U_0(\vec{p}\,'-\vec{p}_i)\chi(\vec{p}_i;\vec{p},\vec{P})\ ,$$

in terms of which

$$\Gamma(\vec{p}\,';\vec{p},\vec{P})=\frac{1}{\Omega}\sum_{p_i}U_0(\vec{p}\,'-\vec{p}_i)\chi(\vec{p}_i;\vec{p},\vec{P})\ .$$

We solve for χ in coordinate space defining ($\hbar\vec{k}=\vec{p}$)

$$\chi_E(\vec{x};\vec{k},\vec{P})=\int\frac{d^3k'}{(2\pi)^3}e^{i\vec{k}'\cdot\vec{x}}\chi_E(\vec{k}\,';\vec{k},\vec{P})\ ,$$

giving

$$\chi_E(\vec{x};\vec{k},\vec{P})=e^{i\vec{k}\cdot\vec{x}}+\int d^3y\left[\int\frac{d^3k_i}{(2\pi)^3}e^{i\vec{k}_i\cdot(\vec{x}-\vec{y})}\times G_2^{\rm HF}(\vec{k}_i;\vec{k},\vec{P})\right]\times U_0(y)\chi_E(y;\vec{k},\vec{P})$$

and

$$\Gamma(\vec{k}\,';\vec{k},\vec{P})=\int d^3x\,e^{-i\vec{k}'\cdot\vec{x}}U_0(x)\chi_E(x;\vec{k},\vec{P})\ . \tag{10}$$

In relative momentum,

$$G_2^{\rm HF}(\vec{k}_i;\vec{k},\vec{P})=\left[\frac{Q_P}{D+i\eta}-\frac{Q_H}{D-i\eta}\right], \tag{11}$$

where

$$Q_P(\vec{k}_i,\vec{P})=\left[1-n\left[\frac{\vec{P}}{2}+\vec{k}_i\right]\right]\left[1-n\left[\frac{\vec{P}}{2}-\vec{k}_i\right]\right]$$

and

$$Q_H(\vec{k}_i,\vec{P})=n\left[\frac{\vec{P}}{2}+\vec{k}_i\right]n\left[\frac{\vec{P}}{2}-\vec{k}_i\right]$$

are the particle- and hole-state Fermi exclusion operators, respectively, and

$$D=\epsilon\left[\frac{\vec{P}}{2}+\vec{k}\right]+\epsilon\left[\frac{\vec{P}}{2}-\vec{k}\right]-\epsilon\left[\frac{\vec{P}}{2}+\vec{k}_i\right]-\epsilon\left[\frac{\vec{P}}{2}-\vec{k}_i\right] \tag{12}$$

is the energy denominator. For the off-energy-shell case, $\epsilon(\frac{1}{2}\vec{P}+\vec{k})$ and $\epsilon(\frac{1}{2}\vec{P}-\vec{k})$ are replaced by an arbitrary energy E and the subscript E on χ reminds us of this possibility.

B. Angle averaging

For $\vec{P}\neq0$, $G_2^{\rm HF}$ depends upon the angle α between $\vec{k}_i$ and $\vec{P}$. Before χ_E can be expanded in partial waves, this dependence must be removed. To do this we simply approximate each Q by a $\bar{Q}$ averaged over the angle α between $\vec{k}_i$ over $\vec{P}$ ($\mu=\cos\alpha$),

$$\bar{Q}(k_i,P)=\tfrac{1}{2}\int_{-1}^{1}d\mu\,\bar{Q}(k_i;P,\mu)\ .$$

We also approximate ϵ in $n(\epsilon)$ by a free-particle spectrum having an m^* given by the calculated m^* at ϵ_F. At low T this should be valid since ϵ near ϵ_F only is important in $n(\epsilon)$. The $\bar{Q}$ have been calculated by Bishop *et al.*,[28]

$$\bar{Q}_P(k_i,P)=\frac{1}{\beta' Pk_i}\{1-\exp[-2\beta'(P^2/4+k_i^2-\mu')]\}^{-1}\times L(k_i,P)\ ,$$
$$\bar{Q}_H(k_i,P)=\frac{1}{\beta' Pk_i}\{\exp[2\beta'(P^2/4+k_i^2-\mu')]-1\}^{-1}\times L(k_i,P)\ , \tag{13}$$

where

$$L(k_i,P)=\ln\left[\frac{\cosh\{\frac{1}{2}\beta'[(\frac{1}{2}P+k')^2-\mu']\}}{\cosh\{\frac{1}{2}\beta'[(\frac{1}{2}P-k')^2-\mu']\}}\right]$$

and $\beta'=(\beta\hbar^2/2m)(m^*)^{-1}$ and $\mu'=\mu(\hbar^2/2m)^{-1}(m^*)^{-1}$ are reduced temperatures and chemical potentials. For $P\neq0$ an angle averaging of the index in $\epsilon(\vec{P}/2\pm\vec{k}_i)$ is also required, for which we used[23]

$$\left[\frac{\vec{P}}{2}\pm\vec{k}_i\right]^2\approx\frac{P^2}{4}+k_i^2\pm\frac{1}{\sqrt{3}}k_iP\ . \tag{14}$$

For $P=0$,

$$Q_P(k_i)=(1+e^{-\beta'(k_i^2-\mu')})^{-2}\ ,$$
$$Q_H(k_i)=(e^{\beta'(k_i^2-\mu')}+1)^{-2}\ . \tag{15}$$

We checked the above approximations by comparing $P=0$ with finite-P results and, in the case of (14), general energy spectrum cases against free-particle spectrum results where angle averaging is not needed, since P cancels between the initial and intermediate states in D. We found (14) was a good approximation in $G_2^{\rm HF}$. Parenthetically, we did, however, find (14) was a poor approximation for indices such as $\vec{k}+\vec{q}$ appearing in the zero-order density-density response function where $\epsilon(\vec{k}+\vec{q})-\epsilon(\vec{k})$ is required.

C. Partial waves

With the above angle averages we expand in partial waves,

$$\chi_E(\vec{x};\vec{k},\vec{P})=\sum_L(2L+1)i^LP_L(\hat{k}\cdot\hat{x})\frac{u_L(kx)}{kx}\ ,$$
$$e^{+i\vec{k}\cdot\vec{x}}=\sum_L(2L+1)i^LP_L(\hat{k}\cdot\hat{x})\frac{I_L(kx)}{kx}\ , \tag{16}$$

where following Østgaard, $j_L = I_L/kx$ is a half-integral-order Bessel function and u_L is the Lth-order wave function we seek.

The equation for u_L is

$$u_L(kx) = I_L(kx) + \int_0^\infty dy\, \gamma_L(x,y) U_0(y) u_L(kx) , \tag{17}$$

where

$$\gamma_L(x,y) = \frac{2}{\pi} \int_0^\infty dk_i I_L(k_i x) I_L(k_i y) G_2^{\mathrm{HF}}(E;k_i,P) . \tag{18}$$

A similar expansion of Γ gives

$$\Gamma(\vec{k}\,';\vec{k},\vec{P}) = \sum_L (2L+1) P_L(\hat{k}'\cdot\hat{k}) \Gamma_L(k';k,P) , \tag{19}$$

where the Lth partial wave is

$$\Gamma_L(k';k,P) = \frac{4\pi}{kk'} \int_0^\infty dx\, I_L(k'x) U_0(x) u_L(kx) . \tag{20}$$

Equations (17), (18), and (20) are exactly those solved by Østgaard,[26] except that the G_2^{HF} in (11) is more general. They are the same, when transformed into the momentum representation, as those solved by Ghassib *et al.*[27] if the $\epsilon(k)$ in G_2^{HF} of (11) are restricted to free-particle energies.

We express our results for the diagonal $\Gamma(k;k,P)$ in terms of the spin-symmetric and spin-antisymmetric components

$$\begin{aligned} \Gamma^s(k;k,P) &= \tfrac{1}{2}(\Gamma^{\uparrow\uparrow} + \Gamma^{\uparrow\downarrow}) = \tfrac{1}{2}(3a_0 + a_e) , \\ \Gamma^a(k;k,P) &= \tfrac{1}{2}(\Gamma^{\uparrow\uparrow} - \Gamma^{\uparrow\downarrow}) = \tfrac{1}{2}(a_0 - a_e) , \end{aligned} \tag{21}$$

where

$$\begin{aligned} a_0(k;k,P) &= \sum_{\substack{L \\ \text{odd}}} (2L+1)\Gamma_L(k;k,P) , \\ a_e(k;k,P) &= \sum_{\substack{L \\ \text{even}}} (2L+1)\Gamma_L(k;k,P) . \end{aligned} \tag{22}$$

In terms of $\Gamma^s(k;k,P)$ the SPE spectrum we use in G_2^{HF} is, at $T=0$ K (Appendix),

$$\epsilon(k) = \frac{P^2}{2m} + \Sigma_1(k) + \Sigma_R(k) , \tag{23}$$

where

$$\Sigma_1(k_1) = \begin{cases} \dfrac{8}{\pi^2} \displaystyle\int_0^{(k_F-k_1)/2} dk\, k^2 \Gamma^s + \dfrac{4}{\pi^2} \int_{(k_F-k_1)/2}^{(k_F+k_1)/2} dk\, k^2 \Gamma^s \left[1 + \dfrac{k_F^2 - 4k^2 - k_1^2}{4kk_1} \right], & k_1 \le k_F \\ \dfrac{4}{\pi^2} \displaystyle\int_{|k_F-k_1|/2}^{|k_F+k_1|/2} dk\, k^2 \Gamma^s \left[1 + \dfrac{k_F^2 - 4k^2 - k_1^2}{4kk_1} \right], & k_1 > k_F \end{cases} \tag{24}$$

and $\Sigma_R(k_1)$ is given by (A6).

The solution of (17)—(20) is straightforward except for $\gamma_L(x,y)$ where two problems arise: (1) $I_L(k_i x)$ is a long-range function of $k_i x$ and (2) the zeros in D must be treated with care. We handled (1), following Østgaard,[26] by adding and subtracting the free-particle $\gamma_L(x,y)$ [$Q_P = 1$, $\epsilon(k) = \hbar^2 k^2/2m$], which may be calculated exactly in both the scattering ($E>0$) and bound ($E<0$) cases. The range of numerical integration can then be short ($0 - \sim k_F$). In the second term of G_2^{HF} no problem arises since Q_H falls off rapidly for $k_i > k_F$. The zeros in D always remain even for complex $\epsilon(k)$ since both the real and imaginary parts of D cancel when $k_i = k$. [In most other examples of this type, e.g., the density-density response function, the zeros disappear when $\epsilon(k)$ has an imaginary part.] The zeros were handled by expanding γ_L in a Taylor's series about its value where the zero occurs and integrating over this region analytically as directed by the sign of $\pm i\eta$. We also found it important to use a complex inversion routine to invert (17) to ensure convergence of the inversion.

D. Units

Throughout, we use ϵ in K and k in Å^{-1} so that Γ emerges in units of K Å^3. For ready comparison of Γ with Landau parameters[13,14] we multiply Γ in K Å^3 by the *observed* density of states per unit volume at the Fermi surface. The Γ presented then have the same dimensionless "units" as Landau parameters, i.e.,

$$\Gamma_L(\text{dimensionless}) = \Gamma_L \left[\frac{dn}{d\epsilon} \right]_{\epsilon_F} ,$$

where, in units of (K Å^3)$^{-1}$,

$$\left[\frac{dn}{d\epsilon} \right]_{\epsilon_F} = \frac{m^* k_F}{\pi^2 \hbar^2} = 0.0153 ,$$

using $m^* = 3.1$.

IV. MODEL SPECTRUM RESULTS

A. Østgaard's model spectrum

As a check, we begin by reproducing the Γ calculated by Østgaard.[26] He retained the first term of G_2^{HF} in (11) only, giving

$$G_2^0 = \frac{Q_P}{\epsilon(1) + \epsilon(2) - \epsilon(5) - \epsilon(6)} . \tag{25}$$

He represented the initial-state energies ϵ_1 and ϵ_2 by a model (reference) spectrum of the form, e.g.,

$$\epsilon_0(1) = A_0 + \frac{\hbar^2}{2Mm_0^*} k_1^2, \quad k_1 < k_F \tag{26}$$

and the intermediate-state energies ϵ_5 and ϵ_6 by free-particle energies, e.g.,

$$\epsilon_i(5)=\frac{\hbar^2 k_5^2}{2M}, \quad k_1 \geq k_F \ . \tag{27}$$

The Q_P guarantees that intermediate-state labels k_5 and k_6 were always greater than or equal to k_F. Various values of the parameters A_0 and m_0^* were selected but they were always chosen so that $\epsilon_1+\epsilon_2 \leq 0$. Since the $\epsilon_5+\epsilon_6$ are always greater than or equal to zero the denominator in G_2^0 is always negative and never vanishes. There is therefore no need to introduce a small imaginary part in G_2^0 and the resulting Γ is also purely real.

Substituting (26) and (27) into (25) and introducing relative momenta [as in (12)] G_2^0 becomes

$$G_2^0=-\frac{Q_P}{\frac{\hbar^2}{M}(\gamma^2+k_i^2)} \ , \tag{28}$$

where

$$\gamma^2=2\Delta k_F^2-\frac{k^2}{m_0^*} \ ,$$
$$\Delta=-\left[\frac{M}{\hbar^2}\right]\frac{A_0}{k_F^2}-\frac{P^2}{4k_F}(m_0^{*-1}-1) \ . \tag{29}$$

Østgaard's model spectra for ϵ_0 and ϵ_i are shown in Fig. 1 for $\Delta=0.4$ and $m_0^*=2.5$, where the gap between ϵ_0 and ϵ_i at $k=k_F$ is displayed.

The effective interaction Γ we obtain here using Østgaard's model spectrum for $\Delta=0.4$, $m_0^*=2.5$, $P=0$, and the Yntema-Schneider[33] potential is displayed in Table I. These agree with the values quoted by Østgaard.[26] In a later paper and using different values of Δ, Østgaard quotes values of the $L=0$ component Γ_0, $\sim 20\%$ less than we found; otherwise all other components agreed.

We note here that the Γ^s obtained using Østgaard's spectrum is ~ 2–3 times smaller (and $\Gamma^a \sim 2$ times larger) than that obtained using the free-particle or a self-consistent energy spectrum (compare Tables I and II). We attribute this difference to the gap between ϵ_0 and ϵ_i at k_F.

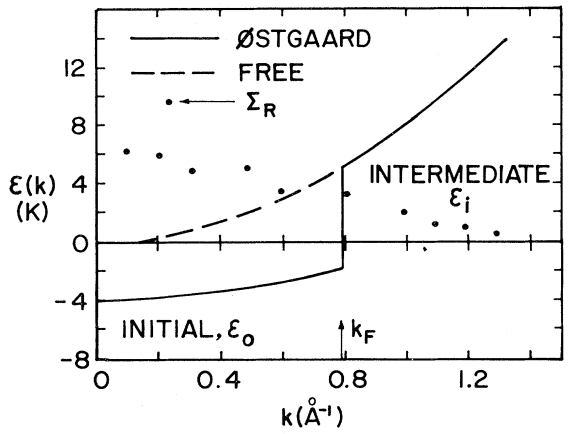

FIG. 1. Østgaard's model SPE spectrum showing the initial- (ϵ_0) and intermediate- (ϵ_i) state energies. The dots are the rearrangement energies Σ_R calculated here using this spectrum.

The Γ^s is also very sensitive to changes in Δ and m_0^* since this changes the gap size at $k=k_F$.

The Γ^s in Table I, when substituted in (7), gives an energy spectrum that agrees well with (26) for $m_0^*=2.5$ and $\Delta=3.1$ at $k_F=0.78$ [Refs. 26(c)]. Thus approximate self-consistency for the input initial state and output spectrum is possible.

B. Rearrangement energies

Østgaard's spectrum provides a convenient and simple form to investigate the rearrangement energy. From the Appendix

$$\Sigma_R(1)=\frac{2k_F^3}{\pi^2}\int_0^1 dx\, x^3\left[\frac{\partial\Gamma^s(x)}{\partial[\ln(1)/N]}\right](1-\tfrac{3}{2}x+\tfrac{1}{3}x^3) \ , \tag{30}$$

where $x=k/k_F$. The Γ^s depends upon $n(1)$ via the exclusion factors $Q_P=[1-n(5)][1-n(6)]$ and $Q_H=n(5)n(6)$ when k_5 and k_6 pass through k_1. If we change n in the region of k_1 this will change the form of

TABLE I. Angular momentum components ($L=0$–5) of the diagonal T matrix calculated using the energy denominator (28) proposed by Østgaard (Ref. 26) for $\Delta=0.4$ and $m_0^*=2.5$, c.m. $P=0$, and the Yntema-Schneider potential. The Γ appear multiplied by the observed density of states per unit volume at $\epsilon_F[(dn/d\epsilon)_{\epsilon=\epsilon_F}=3/(2\Omega_0\epsilon_F)=0.0153$ (K Å^3)$^{-1}$] and are therefore in the unitless "dimensions" of the Landau F parameters. [To convert to K Å^3, divide by $(dn/d\epsilon)_{\epsilon=\epsilon_F}$.] The ^{3}He is at $\Omega_0=61.129$ Å^3 per particle or $k_F=0.785$ Å^{-1}. The values here agree with those quoted in Table III of Østgaard [Ref. 26(e)] [divide Γ here by $(\hbar^2/M)(dn/d\epsilon)_{\epsilon=\epsilon_F}$ ($\hbar^2/M=16.169$ K Å^2) to obtain Γ in units of Å and multiply the odd L by 3]. The Γ^s and Γ^a are the spin-symmetric and spin-asymmetric interactions defined in (21).

k (Å^{-1})	k/k_F	Γ_0	Γ_1	Γ_2	Γ_3	Γ_4	Γ_5	Γ^s	Γ^a
0.1	0.127	4.03	−1.17	−0.033	0	0	0	0.243	−2.58
0.2	0.254	7.11	−3.66	−0.405	−0.028	−0.002	0	−2.18	−5.19
0.3	0.382	10.60	−5.67	−1.39	−0.204	−0.024	−0.002	−4.22	−7.53
0.4	0.509	13.45	−6.19	−2.78	−0.640	−0.134	−0.024	−5.01	−8.69
0.5	0.636	15.15	−5.04	−4.24	−1.299	−0.369	−0.103	−4.40	−8.50
0.6	0.763	15.57	−2.46	−5.45	−2.133	−0.693	−0.257	−2.56	−7.13
0.7	0.891	14.48	1.05	−6.08	−3.124	−1.081	−0.454	0.04	−5.09
0.8	1.108	13.15	4.81	−5.83	−3.909	−1.547	−0.684	2.84	−2.91
0.9	1.145	10.96	8.18	−4.59	−5.077	−2.042	−0.979	5.35	−1.09

TABLE II. Rearrangement energy $\Sigma_R(k)$ vs k evaluated using Østgaard's model spectrum ($m_0^*=2.5$ and $\Delta=0.21$), c.m. $P=0$, and the Yntema-Schneider potential. At $k=0.8$ Å^{-1}, Σ_R was evaluated in two ways (see text).

k (Å^{-1})	$\Sigma_R(k)$ (K)
0.1	6.35
0.2	6.24
0.3	4.77
0.4	6.02
0.5	5.19
0.6	3.52
0.8	3.02
(0.8)	(3.04)
1.0	2.08
1.1	1.27
1.2	1.04
1.3	0.64

Q_P and Q_H. At $T=0$ K, $n(1)$ is unity for $k_1 \leq k_F$ and zero thereafter.

The Σ_R was evaluated in two ways:

(1) Following Brueckner and Goldman[39] the occupation n was increased from unity by a small amount δ around k_1 over a width γ in k space. The resulting change in the number of particles at radius k_1 is

$$\delta n(1)=\frac{V}{(4\pi^3)}4\pi k_1^2\,\delta\gamma$$

compared with a total of

$$N=[V/(4\pi^3)]4\pi k_F^3/3\ .$$

The effective interaction $\Gamma^s(\delta\gamma)$ was computed with this increased occupation and the derivative in the large parentheses in (30) is evaluated as

$$\frac{\delta\Gamma^s}{\delta[n(1)/N]}=\left[\frac{\Gamma^s(\delta\gamma)-\Gamma^s}{\delta\gamma}\right]\frac{k_F}{3}\left[\frac{k_F}{k_1}\right]^2 . \tag{31}$$

For $\gamma=0.03$ Å^{-1} and $\delta=0.05$ (in the actual numerical work Q_P and Q_H were changed by δ) this procedure yielded consistent results which are listed in Table II. These numerical $\Sigma_R(k)$ approximately obey the relations

$$\Sigma_R(k)=\begin{cases}\Sigma_R(k_F)\left[2-\left[\dfrac{k}{k_F}\right]^2\right], & k\leq k_F\\ \Sigma_R(k_F)\left[\dfrac{k_F}{k}\right]^2, & k\geq k_F\ .\end{cases} \tag{32}$$

The relation for $k\leq k_F$ was proposed by Østgaard[26] on the basis of his numerical work. Brueckner and Goldman[39] also found $\Sigma_R(0)\approx 2\Sigma_R(k_F)$, consistent with (32).

(2) For the special case $k_1=k_F$, we may increase $n(1)$ by simply increasing k_F, by, for example, an amount Δk_F. Then

$$\frac{\delta n(k_F)}{N}=\frac{1}{N}\left[\frac{\partial N}{\partial k_F}\right]\Delta k_F=\frac{3}{k_F}\Delta k_F$$

and

$$\frac{\delta\Gamma^s}{\delta[n(k_F)/N]}=\frac{k_F}{3}\frac{\Gamma^s(k_F+\Delta k_F)-\Gamma^s(k_F)}{\Delta k_F}\ .$$

The derivative was evaluated as a finite difference by calculating Γ^s at different values of k_F. The resulting value is $\Sigma_R(k_F)=3.04$ K at $k_F=0.78$ Å^{-1}, which agrees well with the values listed in Table II. Σ_R is sensitive to changes in the energy denominator. For $m_0^*=2.5$ and $\Delta=0.5$, $\Sigma_R(k_F)$ increased by 2. With the use of a free-particle spectrum, $\mathrm{Re}\Sigma_R(k_F)=2.58$ K, and for the fully iterated spectrum $\mathrm{Re}\Sigma_R(k_F)=1.78$ K.

The above Σ_R were all obtained using the BBG approximation (first term of G_2 only retained). For the GF case, $\Sigma_R(k_F)$ was always much smaller; $\mathrm{Re}\Sigma_R(k_F)=-0.6$ K at $\Omega=36.83$ cm^3/mole, $\mathrm{Re}\Sigma_R(k_F)=0.3$ K at $\Omega=25.8$ cm^3/mole, and $\mathrm{Re}\Sigma_R(k_F)\approx 0$ at $\Omega=45$ cm^3/mole using the fully iterated SPE spectrum in Γ. This reflects a cancellation in the changes in the two terms of G_2^{HF} to changes in $n(1)$. We could not find any reason in principle why $\Sigma_R\equiv 0$ in the GF case, but at all volumes Σ_R was small and nearly negligible. In this sense the GF method is simpler and makes the definitions of ϵ from E ($\epsilon\equiv\delta E/\delta n$), and as the energy in the single-particle Green function, more consistent. On the basis of these results we evaluated $\Sigma_R(k_F)$ only and assumed, at each stage of the iteration, that $\Sigma_R(k_1)$ obeyed (32) (both real and imaginary parts).

C. Free-particle spectrum

Ghassib and co-workers[27,28] and Bishop *et al.*[29] have evaluated the GF T matrix (3) using free-particle input energies. Particularly, they investigated carefully $\Gamma(k,kP;E)$ off the energy shell for several values of P, temperature, and liquid density. Off the energy shell

$$E=\epsilon_1+\epsilon_2=E_{\mathrm{rel}}+P^2/4M$$

is taken as a variable. Since for free-particle energies the center of momentum (c.m.) energy $P^2/4M$ cancels between $\epsilon_1+\epsilon_2$ and $\epsilon_3+\epsilon_4$, E_{rel} is the natural energy variable to use. For negative E_{rel} Ghassib *et al.*[27] find a simple pole in the $L=0$ component $\Gamma_0(k;k,P,E)$, independent of k, which at $T=P=0$ and $k_F\approx 0.785$ occurs at $E_{\mathrm{rel}}=-0.16$ Å$^{-2}=-2.6$ K.

We confirm the existence of this singularity. In Fig. 2 we show $\Gamma_0(k;k,P,E)$ calculated here using the Beck potential for $P=T=0$ and negative E_{rel}. Γ_0 clearly has a pole when free-particle energies are used, at $E_{\mathrm{rel}}\approx -1.7$ K for the Beck potential. The pole is, however, softened into a "hump" at a somewhat higher E_{rel} when the self-consistent (complex) $\epsilon(k)$, calculated in the following section, is used for the intermediate states. The pole seems, therefore, to be a property of the free-particle spectrum. The origin of this singularity numerically is not clear. Bishop *et al.*[28] discuss the physical implications of the singularity in some detail. As noted by Bishop *et al.* the BBG Γ_0 does not have a pole. For $E_{\mathrm{rel}}<0$, Γ is purely real.

For $E_{\mathrm{rel}}>0$, Γ is complex, and in analogy with scattering in free space ($Q_P=Q_H=1$), Ghassib *et al.*[27] express their results for the diagonal, on-energy shell Γ_L in terms of a phase shift,

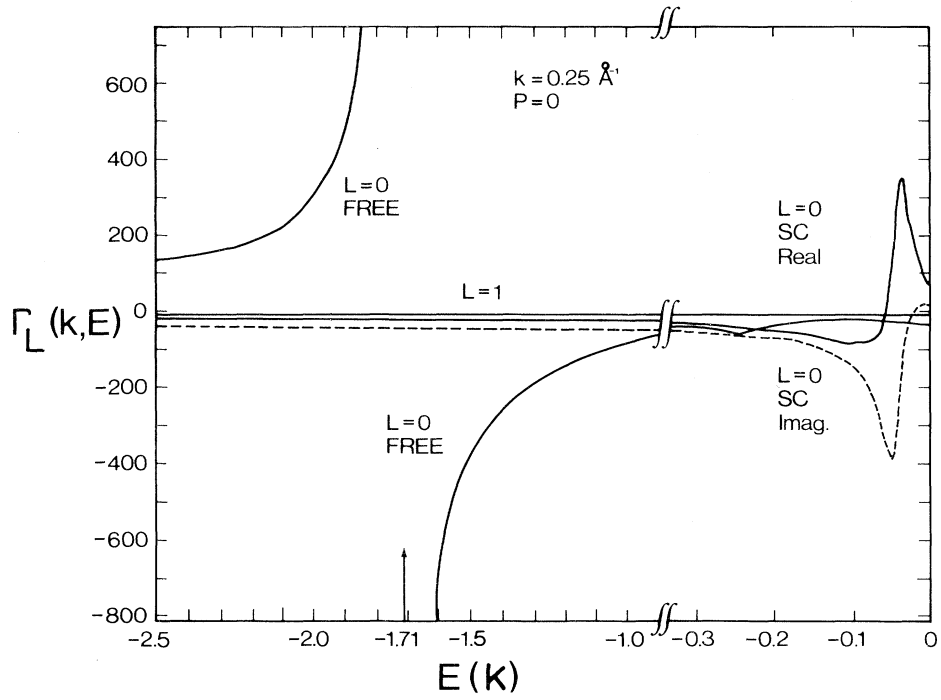

FIG. 2. Galitskii-Feynman $\Gamma_L(k;E)$ at $k=0.25$ Å^{-1} and variable negative (off-shell) relative energy E for $L=0$ and 1. The $L=0$, FREE shows $\Gamma_0(k,E)$ using a free-particle intermediate-state spectrum. In this case Γ_0 is purely real and has a singularity at $E\approx -1.7$ K. The $L=0$, SC shows $\mathrm{Re}\Gamma_0$(—) and $\mathrm{Im}\Gamma_0$(- - -) using the self-consistent intermediate-state spectrum for which there is no singularity. The $L=1$ is the same for each case.

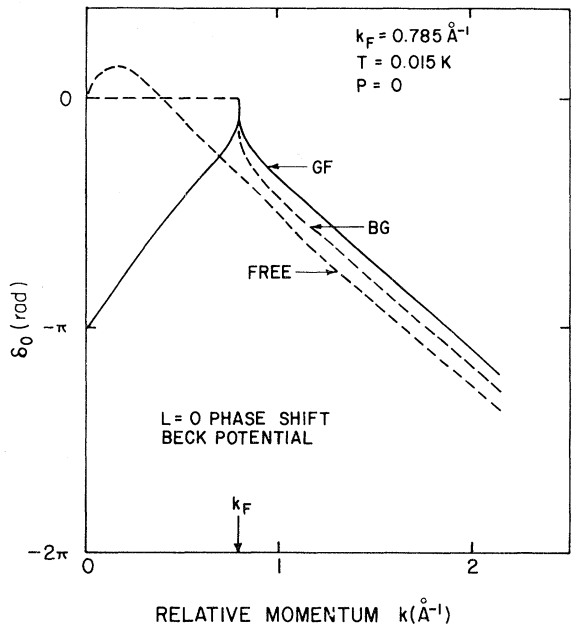

FIG. 3. Phase shift $\tan\delta_0=\mathrm{Im}\Gamma_0/\mathrm{Re}\Gamma_0$ for the GF, the BBG, and free-scattering T matrices for angular momentum $L=0$. A free-particle input energy spectrum is used (diagonal, on-shell energies).

$$\delta_L(k,P,T)=\tan^{-1}\left[\frac{\mathrm{Im}\Gamma_L(k,P,T)}{\mathrm{Re}\Gamma_L(k,P,T)}\right].$$

This is essentially the ratio of the imaginary to real parts of Γ_L. In Fig. 3 we show δ_0 (for the diagonal, on-energy-shell case) obtained here for the GF, the BBG ($Q_H=0$), and the free-space ($Q_P=Q_H=1$) cases. These phase shifts agree well with those calculated by Bishop *et al.*[28] and illustrate nicely the difference between the three cases. In the BBG case $\mathrm{Im}\Gamma_0=0$ for $k\le k_F$ since $Q_P=0$ for $k\le k_F$ at $T=0$ K. In the GF case $\mathrm{Im}\Gamma_0$ for $k\le k_F$ comes entirely from the Q_H term. For both the BBG and GF cases, $\mathrm{Im}\Gamma_0$ is always negative and is zero at $k=k_F$. At large wave vector k, the Fermi statistical exclusion factors affect Γ_0 little.

In Fig. 3 we see that the GF $\delta_0(k)$ rises sharply in a cusp at $k=k_F$. This cusp, shown in more detail in Fig. 4, softens as T is increased. Also in Fig. 4, δ_L for $L=1$ and $L=2$ are shown for the GF case. All these results, calculated using the Beck potential, agree well with Bishop *et al.*[28,29] who used the modified Frost-Musulin (MFM) potential.[29]

In Fig. 5 we show the diagonal, spin-symmetric $\Gamma^s(k,k)$ and spin-antisymmetric $\Gamma^a(k,k)$ T matrices calculated from (21) using a free-particle input spectrum for both initial ($E=\epsilon_1+\epsilon_2$) and intermediate (ϵ_5 and ϵ_6) states in G_2^{HF}. The GF and BBG T matrices differ significantly only for $k\le k_F$. At large k scattering to particle states above k_F dominates and the second term in G_2^{HF} (containing Q_H) becomes negligible. The imaginary part of $\Gamma(k)$

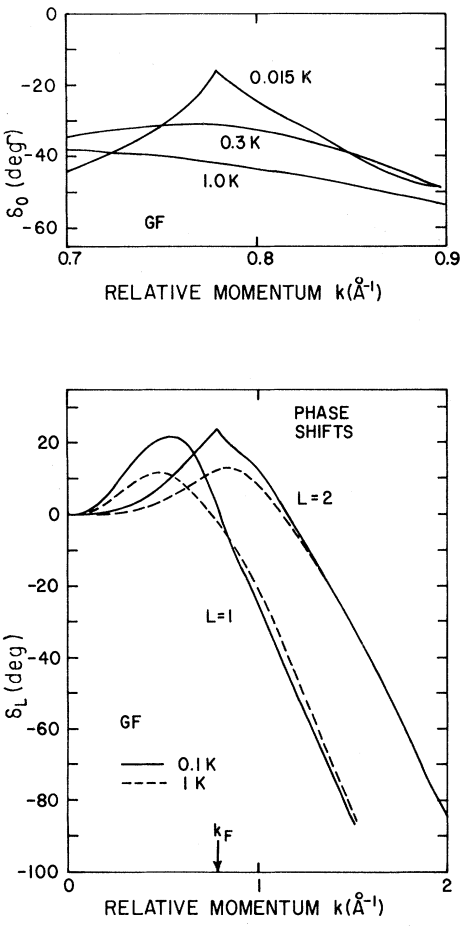

FIG. 4. Same as Fig. 3 for the GF case showing temperature dependence.

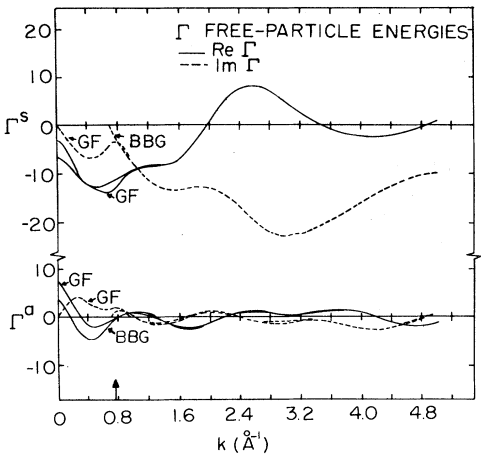

FIG. 5. Spin-symmetric (Γ^s) and spin-antisymmetric (Γ^a)T matrices (diagonal and on-shell) calculated using free-particle energies. The Γ are multiplied by $(dn/d\epsilon)_{\epsilon=\epsilon_F}=m^*k_F/\pi^2\hbar^2$ $=0.0153$ (K Å^3)$^{-1}$ so that they are in the same dimensionless units as the observed Landau parameters. To convert to K Å^3, divide by 0.0153 (K Å^3)$^{-1}$.

is zero in the BBG case for $k \leq k_F$ and this is the most significant difference.

V. SELF-CONSISTENT RESULTS

In this section we present results for liquid ^{3}He fixed at the saturated-vapor-pressure (SVP) volume $\Omega_0=36.83$ cm^3/mole, $k_F=0.785$ Å^{-1}, $T=0$ K, and the c.m. P of all interacting pairs assumed zero.

A. The Γ and $\epsilon(k)$

An internally consistent SPE spectrum $\epsilon(k)$ and corresponding effective interaction $\Gamma(k,k)$ were obtained by iterating between Eq. (3) for Γ and Eq. (6) for $\epsilon(k)$. The iterations were started by using a free-particle input energy spectrum in $G_2^{\rm HF}$. The resulting Γ^s was used to calculate $\epsilon(k)$ from (23). This $\epsilon(k)$ was then inputted into $G_2^{\rm HF}$ and this procedure iterated until consistent. The spectra $\epsilon(k)$ obtained on the way toward convergence are shown in Fig. 6 for the GF case. Typically, six to seven iterations were required to refine $\epsilon(k)$ in detail. However, Fig. 6 shows that even the first order $\epsilon(k)$ (labeled 1) was quite close to the final $\epsilon(k)$. This shows that $\Gamma^s(k,k)$ is not greatly sensitive to the input spectrum, provided it is continuous. The starting free particle $\epsilon(k)$ (labeled 0) and the final $\epsilon(k)$ (labeled F) differ chiefly by a constant shift in energy. This difference largely cancels between $\epsilon_1+\epsilon_2$ and $\epsilon_5+\epsilon_6$ in $D=\epsilon_1+\epsilon_2-\epsilon_5-\epsilon_6$, making $\Gamma(k)$ insensitive to this sort of change in $\epsilon(k)$.

The final self-consistent (SC) spectrum $\epsilon(k)$ for the BBG and GF cases is shown in Fig. 7. The dashed line marked R in Fig. 7 is the rearrangement energy contribution $\Sigma_R(k)$ to $\epsilon(k)$ in the BBG case. As noted in Sec. III,

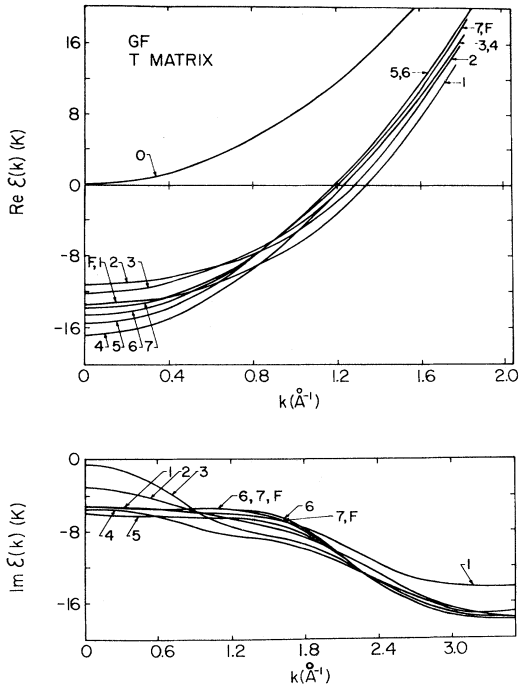

FIG. 6. Variation of energy spectrum during iteration for GF effective interaction; 0 is the starting $\epsilon(k)$, F is the final $\epsilon(k)$.

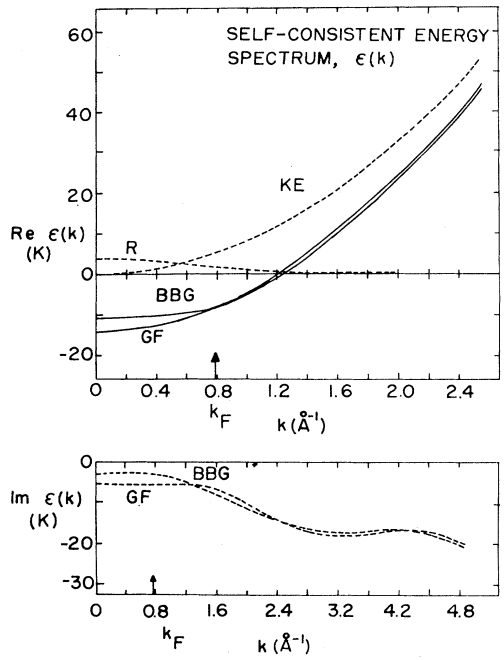

FIG. 7. Self-consistent energy spectrum obtained using the GF and BBG T matrices. The dashed line R is the rearrangement energy Σ_R in the BG case. $\Sigma_R \approx 0$ in the GF case.

Σ_R is small ($\lesssim 0.5$ K) in the GF case. The difference between the $\epsilon(k)$ in the GF and BBG cases is due chiefly to Σ_R; neglecting Σ_R the real parts of the two $\epsilon(k)$ would have been essentially the same. The imaginary part of $\epsilon(k)$ for $k \lesssim 1.5k_F$ is greater in magnitude in the GF case due to the hole-state contributions.

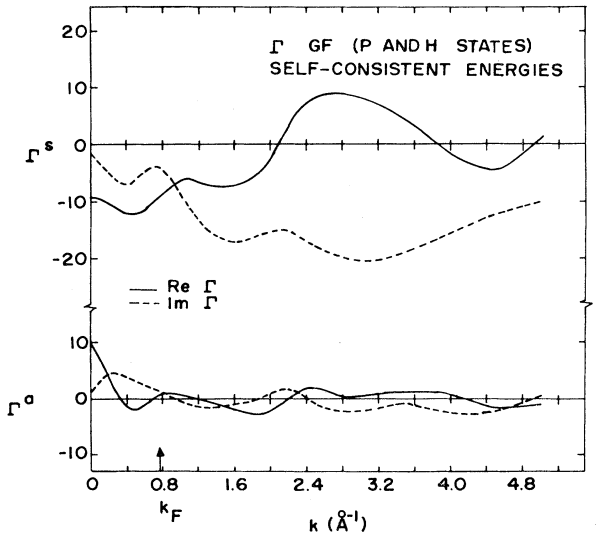

FIG. 8. Spin-symmetric (Γ^s) and spin-antisymmetric (Γ^a) T matrices (diagonal and on-shell) using the self-consistent energy spectrum for the GF case. The Γ is shown multiplied by $(dn/d\epsilon)_{\epsilon=\epsilon_F} = m^* k_F/\pi^2\hbar^2 = 0.0153$ (K Å^3)$^{-1}$ so that it is in the same dimensionless units as the observed Landau parameters.

TABLE III. Self-consistent single-particle energy spectrum $\epsilon(k)$ (in K) obtained from (6) using the BBG and GF T matrices.

	BBG T matrix		GF T matrix	
k (Å^{-1})	Reϵ	Imϵ	Reϵ	Imϵ
0.0	−10.72	−4.27	−13.69	−5.47
0.1	−10.69	−4.27	−13.61	−5.49
0.2	−10.61	−4.28	−13.37	−5.53
0.3	−10.46	−4.30	−12.97	−5.58
0.4	−10.22	−4.33	−12.40	−5.62
0.5	−9.90	−4.36	−11.62	−5.63
0.6	−9.46	−4.37	−10.58	−5.60
0.7	−8.88	−4.38	−9.33	−5.54
0.8	−8.12	−4.51	−7.88	−5.48
0.9	−6.97	−4.90	−6.30	−5.43
1.0	−5.44	−5.34	−4.52	−5.37
1.1	−3.58	−5.85	−2.52	−5.34
1.2	−1.40	−6.39	−0.27	−5.40
1.3	1.04	−6.99	2.23	−5.55
1.4	3.71	−7.62	4.95	−5.84
1.5	6.57	−8.28	7.88	−6.24
1.6	9.64	−8.95	10.97	−6.80
1.7	12.88	−9.62	14.19	−7.48
1.8	16.22	−10.35	17.52	−8.29
1.9	19.63	−11.09	20.93	−9.21
2.0	23.14	−11.84	24.41	−10.19
2.1	26.78	−12.58	27.98	−11.20
2.2	30.47	−13.28	31.65	−12.19
2.3	34.30	−13.95	35.42	−13.17
2.4	38.25	−14.61	39.27	−14.07
2.5	42.36	−15.25	43.23	−14.89
2.6	46.61	−15.86	47.31	−15.62
2.7	51.01	−16.40	51.54	−16.25
2.8	55.59	−16.87	55.95	−16.76
2.9	60.35	−17.25	60.56	−17.16
3.0	65.31	−17.53	65.40	−17.45
3.6	93.73	−17.58	93.35	−17.54
4.0	128.72	−16.78	128.09	−16.63
4.5	168.79	−18.02	168.22	−17.52
5.0	211.83	−21.51	210.21	−21.02

The SC $\epsilon(k)$ lies $\sim$10—13 K below zero for $k \lesssim k_F$. This suggests strong binding. The Re$\epsilon(k)$ are smooth and approach the free-particle spectrum (dashed line) at $k \sim 4k_F$. The values of the SC $\epsilon(k)$ are listed in Table III. The T matrices $\Gamma(k)$, calculated using the SC $\epsilon(k)$, are shown in Figs. 8 and 9. Shown are the diagonal ($k'=k$) and on-energy-shell values of the spin-symmetric $\Gamma^s(k)$ and the spin-antisymmetric $\Gamma^a(k)$ T matrices. They are in the dimensionless units used by Landau, i.e., the Γ in K Å^3 are shown multiplied by $(dn/d\epsilon)_{\epsilon=\epsilon_F} = 0.0153$ (K Å^3)$^{-1}$.

Comparing Figs. 5 and 8 we see that the Γ^s and Γ^a calculated using the free-particle spectrum and using the SC spectrum differ little. This emphasizes that Γ is rather insensitive to the input spectrum used, provided the spectrum is continuous and, as here, the two input spectra differ chiefly by a constant shift in energy, independent of k. Comparing Figs. 8 and 9 we see that the GF and BBG T matrices differ little. The only significant difference is at $k \lesssim 2k_F$, and there chiefly in the imaginary part.

To get a physical picture of the Γ^s and Γ^a, we Fourier transformed the real parts to obtain an "effective" (local) potential in real space. The approximate Fourier

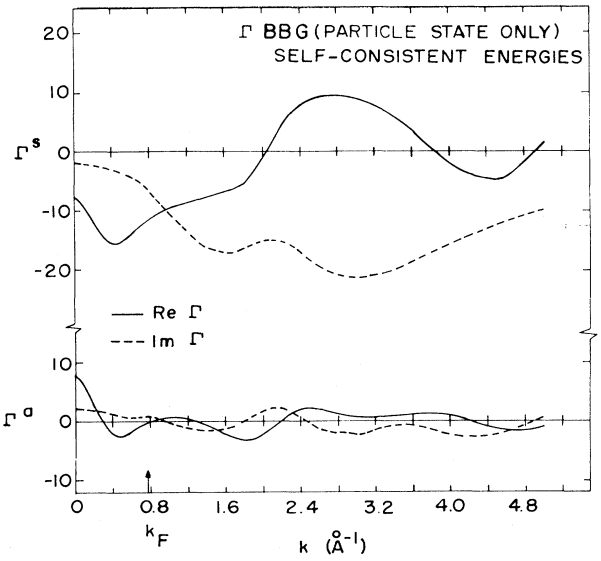

FIG. 9. Same as Fig. 8 for the BBG T matrix.

transform of $\mathrm{Re}\Gamma^s(k)$ [denoted $V^s(r)$] is shown in Fig. 10. As expected the $V^s(r)$ has the hard core removed and is "finite" at $r=0$. It also has a shallow potential minimum and is of short range. The dashed line [$V^s(k)$] in Fig. 10 shows the actual Fourier transform of $V^s(r)$ and a comparison of $V^s(k)$ with $\mathrm{Re}\Gamma^s(k)$ in Fig. 8 gives an indication of the approximate nature of $V^s(r)$. We emphasized fitting the small-k behavior of $\mathrm{Re}\Gamma^s(k)$ to obtain $V^s(r)$ since the long-range behavior of $\mathrm{Re}\Gamma^s(k)$ can eventually be fitted by a single constant, a phase shift.

The approximate Fourier transform of $\mathrm{Re}\Gamma^a(k)$, $V^a(r)$, is shown in Fig. 11. $V^a(r)$ is very shallow and of long range as is anticipated for the spin-dependent interaction. Again $V^a(r)$ is only approximate and was simply cut off at $r\sim 10$ Å. More precision is not meaningful since neither Γ^s nor Γ^a can be well represented by a local potential in any case.[8,22]

The values of the SC T matrix for the BBG and GF cases (as shown in Figs. 8 and 9) are listed in Table IV. The individual angular momentum components of the GF

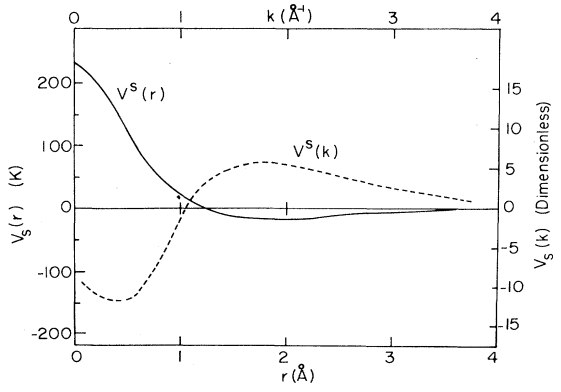

FIG. 10. $V^s(r)$, approximate Fourier transform (FT) of GF $\Gamma^s(k)$. $V_s(k)$, actual inverse FT of $V_s(r)$. Comparison of $V^s(k)$ and $\Gamma^s(k)$ (Fig. 8) displays approximate nature of $V^s(r)$.

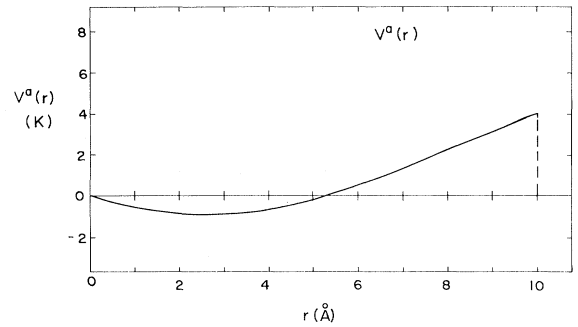

FIG. 11. Approximate Fourier transform GF $\Gamma^a(k)$.

T matrix (see Fig. 12) are listed in Table V.

B. The total energy and $\epsilon(k)$

In Fig. 12 we compare the present $\mathrm{Re}\epsilon(k)$ for low k with previous $\epsilon(k)$. The present $\mathrm{Re}\epsilon(k)$ may be written in the form

$$\mathrm{Re}\epsilon(k)=\epsilon_F\left[\frac{k}{k_F}\right]^2+\mathrm{Re}\Sigma(k)\ ,$$

where $\mathrm{Re}\Sigma(k)$ is the real part of the self-energy including the rearrangement energy and $\epsilon_F\approx 5.0$ K. We see that the present $\mathrm{Re}\epsilon(k)$ lie substantially below the SC Brueckner-Gammel[23] $\epsilon(k)$ and the model spectrum devised by Østgaard.[26] Clearly, the $\Sigma(k)$ calculated by Brueckner and Gammel and by Østgaard is significantly smaller in magnitude [$\Sigma(k)<0$] than we obtain using a continuous input $\epsilon(k)$ spectrum to the T matrix. We return to this point below.

The total energy may be readily calculated using $\mathrm{Re}\Sigma(k)$ as

$$E=\tfrac{3}{5}\epsilon_F+\frac{3}{k_F^3}\int_0^{k_F}dk\,k^2[\tfrac{1}{2}\mathrm{Re}\Sigma(k)]\ .$$

The E we obtain, compared with others, is shown in Table VI. As expected [from the larger, negative $\Sigma(k)$] we find total energies substantially below those found by Brueckner and Gammel and by Østgaard. We find very strong binding approximately 1 K below the observed value of -2.5 K. This difference arises because we have used a continuous $\epsilon(k)$, without a gap at k_F, as we now show.

The $\Sigma(k)$ for $k<k_F$ depends upon Γ^s for $k\le k_F$. The $\Gamma^s(k)$ calculated by Østgaard and calculated here in the GF case are compared in Fig. 13(b). Clearly the present SC GF $\Gamma^s(k)$ has larger negative values at low k by a factor of order 2—3. We may simulate a gap in the spectrum by doing an off-energy-shell calculation in which the initial-state energies are fixed at a constant low energy $E=\epsilon_1+\epsilon_2$. The intermediate states remain given by the SC $\epsilon(k)$. If we set E below the present SC spectrum, this simulates an initial-state spectrum that lies below the intermediate-state spectrum. An $E\approx -20$ K is required to simulate the gap used by Østgaard. In Fig. 13(a), we see that the present $\Gamma^s(k)$ increases as E is lowered until at $E\approx -20$ K it is very comparable to the $\Gamma^s(k)$ obtained by Østgaard.

TABLE IV. Diagonal, on-energy-shell T matrices [multiplied by $(dn/d\epsilon)_{\epsilon=\epsilon_F}=0.0153$ (K Å^3)$^{-1}$] vs incoming relative wave vector k. Listed are the spin-symmetric (Γ^s) and spin-antisymmetric (Γ^a) T matrices for the BBG and GF cases. To convert Γ to K Å^3 units, divide by 0.0153 (K Å^3)$^{-1}$.

k	BBG T matrix				GF T matrix			
(Å^{-1})	ReΓ^s	ImΓ^s	ReΓ^a	ImΓ^a	ReΓ^s	ImΓ^s	ReΓ^a	ImΓ^a
0.0	−7.63	−2.07	7.63	2.07	−9.42	−1.37	9.42	1.37
0.1	−8.94	−2.11	6.11	1.96	−9.36	−3.29	7.08	3.24
0.2	−11.78	−2.39	2.74	1.81	−10.36	−5.15	3.39	4.65
0.3	−14.41	−2.67	−0.37	1.43	−11.42	−6.40	0.41	4.77
0.4	−15.57	−3.08	−2.39	1.10	−12.15	−6.96	−1.40	4.04
0.5	−15.45	−3.56	−2.82	0.72	−12.25	−6.48	−2.10	3.17
0.6	−14.32	−4.14	−1.98	0.58	−11.64	−4.90	−1.50	2.57
0.7	−12.93	−5.10	−0.41	0.50	−10.05	−3.58	0.04	1.90
0.9	−9.68	−8.95	0.52	0.16	−7.87	−6.32	0.64	0.56
1.0	−8.82	−10.39	0.30	−0.65	−6.38	−8.96	0.42	−0.37
1.1	−8.00	−11.67	0.02	−1.11	−5.70	−11.20	−0.15	−1.11
1.2	−7.21	−12.99	−0.63	−1.55	−6.41	−13.26	−0.39	−1.79
1.3	−8.33	−15.34	−0.14	−1.42	−7.10	−15.19	−0.41	−1.29
1.4	−7.83	−16.07	−0.71	−1.57	−7.39	−16.14	−0.93	−1.24
1.5	−7.43	−16.77	−1.53	−1.57	−7.24	−16.85	−1.40	−0.93
1.6	−6.94	−17.27	−2.31	−1.38	−6.96	−17.25	−1.83	−0.77
1.7	−6.49	−17.20	−2.90	−0.88	−6.61	−17.10	−2.34	−0.56
1.8	−5.60	−16.53	−3.34	−0.06	−5.84	−16.48	−2.73	−0.13
1.9	−3.89	−15.81	−3.15	0.76	−4.27	−16.02	−2.68	0.35
2.0	−1.75	−15.37	−2.45	1.47	−2.50	−15.59	−2.32	0.98
2.1	0.99	−14.69	−1.32	1.98	0.52	−14.42	−1.43	1.69
2.2	3.97	−15.09	−0.07	2.00	3.28	−14.71	−0.13	1.86
2.3	6.35	−16.39	1.14	1.35	5.83	−15.92	1.09	1.33
2.4	7.85	−18.33	2.00	0.49	7.59	−17.61	1.89	0.34
2.5	8.53	−20.21	2.12	−0.59	8.45	−19.41	2.01	−0.87
3.5	4.50	−19.69	0.82	−0.63	4.59	−19.70	1.03	−0.67
4.0	−1.93	−15.95	0.99	−2.32	−1.63	−15.77	0.90	−2.47
4.5	−5.08	−12.58	−1.62	−2.39	−4.66	−12.47	−1.73	−2.26
5.0	1.11	−10.07	−1.12	0.37	1.16	−10.16	−1.03	0.46

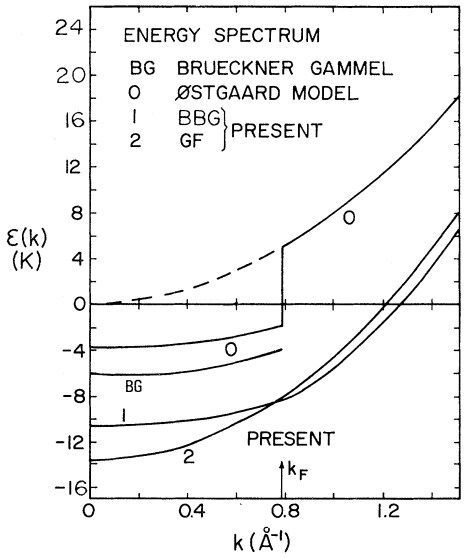

FIG. 12. SPE spectra: PRESENT, calculated here using BBG and GF T matrices; BG, calculated by Brueckner and Gammel; 0 denotes Østgaard's model input spectrum.

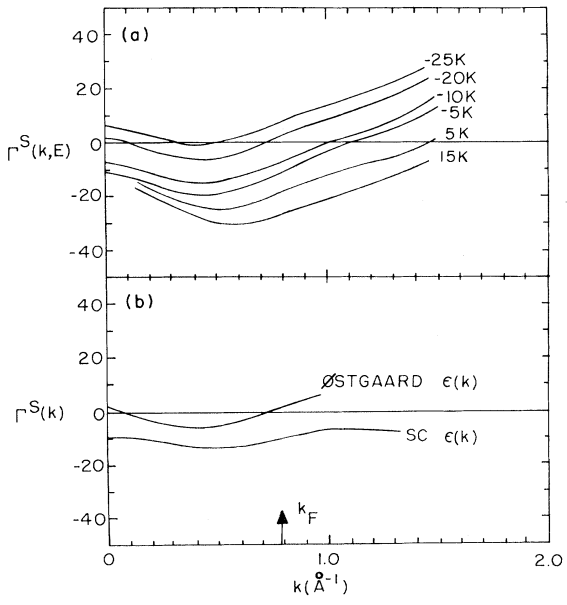

FIG. 13. (a) Upper $\Gamma^s(k,E)$ vs k for fixed off-shell energies $E=-25$ to 15 K in the GF case with the present SC energies as intermediate-state energies. An $E\approx-20$ K simulates the Østgaard model spectrum approximately. (b) Lower $\Gamma^s(k)$ using Østgaard model and present SC energy spectrum (GF T matrix).

TABLE V. Angular momentum components (20) of the diagonal GF T matrix. Units as in Table IV.

k	$\mathrm{Re}\Gamma_L(k,k)$						$\mathrm{Im}\Gamma_L(k,k)$					
($\mathrm{\AA}^{-1}$)	$L=0$	$L=1$	$L=2$	$L=3$	$L=4$	$L=5$	$L=0$	$L=1$	$L=2$	$L=3$	$L=4$	$L=5$
0.0	−18.83	−0.00	−0.00	−0.00	−0.00	−0.00	−2.73	−0.00	−0.00	−0.00	0.0	0.0
0.1	−15.26	−1.14	−0.04	−0.00	−0.00	−0.00	−6.51	−0.03	−0.00	−0.00	0.0	0.0
0.2	−9.84	−3.45	−0.43	−0.03	−0.00	−0.00	−9.55	−0.25	−0.00	−0.00	0.0	0.0
0.3	−4.84	−5.27	−1.45	−0.23	−0.03	−0.00	−10.31	−0.81	−0.04	−0.00	0.0	0.0
0.4	−0.98	−6.04	−2.84	−0.71	−0.15	−0.03	−9.34	−1.45	−0.20	−0.01	0.0	0.0
0.5	1.75	−5.61	−4.30	−1.45	−0.42	−0.12	−7.46	−1.61	−0.54	−0.04	0.0	0.0
0.6	2.93	−3.84	−5.71	−2.43	−0.79	−0.29	−5.20	−1.03	−1.10	−0.14	0.0	0.0
0.7	2.99	−0.75	−6.84	−3.73	−1.24	−0.52	−2.65	−0.47	−1.98	−0.38	0.0	0.0
0.9	2.15	3.60	−4.71	−6.09	−2.33	−1.13	−2.32	−1.43	−1.67	−1.46	0.0	0.0
1.0	1.45	4.56	−2.48	−6.00	−2.79	−1.54	−3.02	−2.95	−0.91	−1.71	0.0	0.0
1.1	0.65	4.61	−0.31	−5.52	−2.97	−2.01	−3.27	−4.43	−0.66	−1.73	0.0	0.0
1.2	0.81	4.08	1.65	−4.67	−5.08	−2.81	−1.90	−5.78	−0.99	−1.50	−1.06	−0.25
1.3	−0.80	3.10	3.22	−3.40	−5.36	−3.45	−2.52	−6.71	−1.83	−1.11	−1.30	−0.42
1.4	−1.28	1.80	4.25	−1.91	−5.27	−4.05	−1.80	−7.24	−3.02	−0.82	−1.39	−0.63
1.5	−1.39	0.55	4.68	−0.34	−4.82	−4.54	−1.45	−7.26	−4.28	−0.77	−1.30	−0.86
1.6	−1.32	−0.84	4.62	1.28	−4.04	−4.84	−0.87	−6.91	−5.54	−1.05	−1.06	−1.06
1.7	−0.87	−2.14	4.03	2.55	−2.96	−4.89	−0.16	−6.04	−6.80	−1.62	−0.75	−1.17
1.8	−0.41	−3.11	3.20	3.50	−1.62	−4.68	0.09	−4.76	−7.63	−2.41	−0.50	−1.14
1.9	0.04	−3.53	2.13	4.22	−0.27	−4.17	0.07	−3.44	−8.15	−3.45	−0.45	−0.94
2.0	0.39	−3.58	0.80	4.56	1.04	−3.40	−0.12	−2.13	−8.53	−4.52	−0.62	−0.66
2.1	0.60	−2.60	−0.47	4.55	2.29	−2.40	−0.27	−0.39	−8.42	−5.62	−1.04	−0.36
2.2	0.66	−1.38	−2.24	4.30	3.41	−1.34	−0.44	0.39	−7.96	−6.65	−1.74	−0.17
2.3	0.67	−0.06	−3.68	3.69	4.29	−0.17	−0.60	0.45	−6.72	−7.64	−2.63	−0.10
2.4	0.68	0.96	−4.62	2.71	4.90	1.07	−0.77	0.06	−4.86	−8.47	−3.68	−0.23
2.5	0.64	1.54	−4.64	1.34	5.22	2.35	−0.84	−0.47	−2.67	−9.07	−4.90	−0.60
3.5	0.11	−0.87	2.85	0.53	−2.21	3.15	0.04	−1.62	−3.36	0.20	−5.53	−8.76
4.0	0.43	0.07	−1.29	2.96	−1.30	3.40	−0.44	0.10	−3.48	−2.69	−0.27	−6.53
4.5	−0.15	0.91	−1.78	−0.61	2.21	−3.49	−0.73	−1.19	−0.42	−5.15	−1.69	−1.03
5.0	−0.28	−0.08	1.00	−1.92	1.41	2.07	−0.26	−1.80	−0.54	−2.22	−4.96	−0.83

TABLE VI. Total energy of liquid ^{3}He calculated by different methods.

Type/Author	Energy (K)	Volume r_0 (Å)	k_F (Å^{-1})
T matrix			
Brueckner-Gammel[a]	−0.96	2.60	0.74
Østggard[b] 2-body	+0.45		
2 + 3-body	−1.0	2.50	0.77
Present GF	−3.7	2.44[c]	0.79
BBG	−3.2	2.44[c]	0.79
Variational			
Schmidt, Lee, Kalos, Chester[d]			
(1) Jastrow-Slater wave function	−2.0	2.40	0.80
(2) Green-function Monte Carlo	−2.2	2.44	0.79
Schmidt and Pandharipande[d]			
Jastrow + 3-body	−2.0	2.44	0.79
Observed[e]	−2.5	2.44	0.79

[a]Reference 23.
[b]Reference 26.
[c]Fixed at observed volume.
[d]Reference 16.
[e]Reference 40.

From this we conclude that a substantially lower $\Gamma^s(k)$, $\mathrm{Re}\epsilon(k)$, and total energy is obtained using a continuous $\epsilon(k)$ rather than one with a gap at k_F in it. Lejeune and Mahaux[37] have found similar lower total energies using a continuous $\epsilon(k)$ for model potentials describing nuclear matter. It is the presence of the gap that is important since either lowering or raising the whole of $\epsilon(k)$ has little effect.

Since we find stronger binding than obtained by Brueckner and Gammel and by Østgaard, we expect to find that E here has its minimum at a smaller volume. Indeed, in Fig. 14 we see the GFHF energy (2) takes its minimum value of $E \approx -4.7$ K at a volume 25 cm^3/mole. This is substantially smaller than the observed[40] SVP (zero pressure) volume of 36.83 cm^3/mole. In real liquid ^{3}He an applied pressure of 30 atm is required to reduce the volume to 25.86 cm^3/mole. Clearly, collective effects, such as are included in the variational calculations of Schmidt *et al.*,[16] must be included in a GFHF theory to predict saturation correctly. At the smallest volumes, iteration of (3), (4), and (6) did not converge well and this is the origin of the large error bars in E of Fig. 14. At the present level the GFHF predicts substantially too much binding.

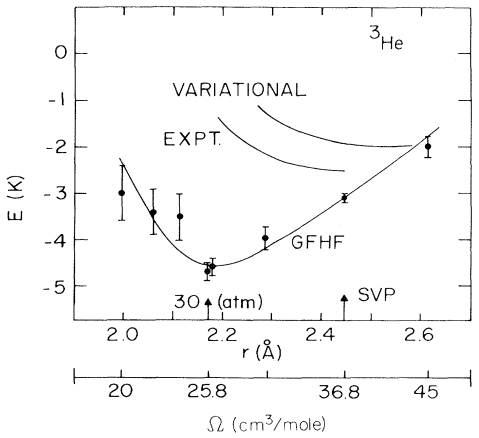

FIG. 14. Ground-state energy E of liquid ^{3}He as calculated here (GFHF), variationally [Schmidt *et al.* (Ref. 16)], and as observed (EXPT) (Ref. 40). The arrows indicate the observed volumes at SVP and at 30 atm pressure.

C. Landau parameters

The effective interaction between quasiparticles appearing in Landau's theory of Fermi liquids is often divided into a direct part and an induced part.[14,15,22] The direct part is assumed to arise chiefly from the interaction of the pair via the hard core of the bare potential. The induced part describes the interaction via the collective excitations, the zero-sound modes and spin fluctuations. In most recent calculations,[8] the induced part is defined as those interaction terms connected by a single induced particle-hole pair excitation and the direct part is the remainder. The present GFHF approximation, which incorporates the bare pair interaction to all orders but no collective effects, should provide a good estimate of the direct part. It will also be interesting to compare results for this approximation using the present continuous single-particle excitations with those obtained by Østgaard using a spectrum having a gap.

The Landau parameter describing the interaction between a quasiparticle in state k_1 having spin σ_1 and one in state k_2 having spin σ_2 is defined as[13,14]

$$f_{\sigma_1\sigma_2}(k_1,k_2)\equiv\frac{\delta^2 E}{\delta n_{\sigma_1}(1)\delta n_{\sigma_2}(2)} . \tag{33}$$

Substituting the HF energy E and differentiating with respect to the explicit factors of $n(1)$ and $n(2)$ in (2), we obtain the lowest-order T-matrix approximation

$$f_{\sigma_1\sigma_2}(k_1,k_2)=\Gamma(k_{12};k_{12})-\delta_{\sigma_1\sigma_2}\Gamma(-k_{12};k_{12}) . \tag{34}$$

This is lowest order because we have ignored any dependence of Γ on n. Including this dependence leads to the rearrangement terms discussed, for example, by Østgaard[26] and by Bertsch.[41] These rearrangement terms begin to incorporate the collective response of the liquid. We seek only the direct interaction here.

From (34), the two spin possibilities are

$$\begin{aligned} f_{\uparrow\uparrow}&=\Gamma(k_{12},k_{12})-\Gamma(-k_{12},k_{12})=2a_0 , \\ f_{\uparrow\downarrow}&=\Gamma(k_{12},k_{12})=a_0+a_e , \end{aligned} \tag{35}$$

where a_0 and a_e are the sums over odd and even angular momentum components of Γ defined in (22). The spin-symmetric and spin-antisymmetry parameters are then

$$\begin{aligned} f^s&\equiv\tfrac{1}{2}(f_{\uparrow\uparrow}+f_{\uparrow\downarrow})=\tfrac{1}{2}(3a_0+a_e) , \\ f^a&\equiv\tfrac{1}{2}(f_{\uparrow\uparrow}-f_{\uparrow\downarrow})=\tfrac{1}{2}(a_0-a_e) . \end{aligned} \tag{36}$$

Introducing the usual dimensionless parameters F which have the same units we have selected for Γ, we see, comparing (36) and (21),

$$F^{s,a} \equiv \left[\frac{dn}{d\epsilon}\right]_{\epsilon=\epsilon_F} f^{s,a} = \Gamma^{s,a} . \tag{37}$$

This sets the spin components of Γ. We now need to specify the relative (k_{12}) and total momentum P to fix the diagonal Γ in (37). The Landau parameters are defined for k_1 and k_2 on the Fermi surface, $|k_1| = k_F$, $|k_2| = k_F$. The k_1 and k_2, therefore, differ only by the angle θ between them ($0 \le \theta \le \pi$). From simple geometry,

$$\begin{aligned} k &= k_{12} = \tfrac{1}{2}|k_1 - k_2| = k_F \sin\tfrac{1}{2}\theta , \\ P &= k_1 + k_2 = 2k_F \cos\tfrac{1}{2}\theta . \end{aligned} \tag{38}$$

In this limit F and $\Gamma(k_{12},P)$ in (37) depend only on the single variable θ,

$$F^{s,a}(\theta) = \Gamma^{s,a}(\theta) . \tag{39}$$

In this case $P \neq 0$, and this is the only instance here where we have used a finite c.m. P. The Landau parameters are expanded in angular momentum components F_L defined by

$$F^{s,a}(\theta) = \sum_L P_L(\cos\theta) F_L^{s,a} , \tag{40}$$

which can be obtained from $F^{s,a}(\theta)$ as

$$F_L^{s,a} = \frac{2L+1}{2} \int_0^\pi d\theta \sin\theta P_L(\cos\theta) \Gamma^{s,a}(\theta) . \tag{41}$$

The $F_L^{s,a}$, we find, using the Galitskii-Feynman $\Gamma^{s,a}(\theta)$ with the SC $\epsilon(k)$ of Fig. 7 as input, are listed in Table VII. These can be understood as follows. In (41), as θ goes from 0 to π, k goes from 0 to k_F. The F_L^s, for example, are therefore "Legendre" moments of the $\Gamma^s(k)$ from 0 to k_F. F_0^s is first the average of $\Gamma^s(k)$ modulated by $\sin\theta$, which emphasizes $\Gamma^s(k)$ in the region $k \approx k_F/\sqrt{2}$. Since $\Gamma^s(k)$ is negative (and large in magnitude), F_0^s will be negative (and large in magnitude). The $\Gamma^s(k)$ must be negative to obtain a bound liquid. In this case a negative F_0^s is inevitable from a HF approximation to zeroth order. The higher moments are less transparent and depend upon the curvature in $\Gamma^s(k)$ [$F_L = 0$ for $L \ge 1$ for constant $\Gamma^s(k)$]. Accuracy also becomes a problem at higher L and the F_L for $L \ge 3$ in Table VII are accurate to ± 0.5 only. The F_0^a is negative because $\Gamma^a(k)$ dips below zero in the region $k \sim 0.7 k_F$ (see Fig. 8).

The calculated F should obey[13] the "forward scattering sum rule"

$$\sum_L (F_L^s + F_L^a) = 0 . \tag{42}$$

The F in Table VII would satisfy (42) if we took $F_L = 0$ for $L \ge 4$ and suggests that the F_L for $L \ge 3$ are not very accurate, as noted above.

In discussing the Landau parameters we note firstly that the present GF T-matrix values in Table VII should represent the direct part of the effective interaction well. We do not expect them to agree with the observed Landau parameters. The general character is that the direct parts of F_0^s and F_0^a are strongly negative. In order to satisfy (42), the direct parts at its higher L cannot vanish. This general character is also obtained by Østgaard[26] and is therefore independent of the input SPE excitation spectrum. Clearly, the induced interaction must compensate greatly, particularly at higher L. Improved values of F can be obtained in the HF approximation by including rearrangement terms, but from Table VII the higher-L components clearly remain large.

Secondly, for the liquid to be mechanically stable against density fluctuations and to ferromagnetic ordering we must have $F_0^s > -1$ and $F_0^a > -1$, respectively.[14,15] For this reason the present direct interaction components may not make a good starting point for a perturbative calculation of the induced interaction. An iterative solution combining the direct and induced parts will probably be required.

D. The effective mass

In Fermi-liquid theory the effective mass of a ^{3}He quasiparticle is defined in terms of the SPE spectrum as

$$\frac{1}{M^*} \equiv \frac{1}{\hbar^2 k} \frac{\partial \epsilon}{\partial k} . \tag{43}$$

The bare mass is just

$$\frac{1}{M} = \frac{1}{\hbar^2 k} \frac{\partial T_k}{\partial k} . \tag{44}$$

The present HF SPE spectrum is

$$\epsilon(k_1, E) = T_k + \Sigma(k_1, E) \tag{45}$$

TABLE VII. Landau parameters in ^{3}He at $\Omega = 36.83$ cm^3/mole.

	Present GF	Present T matrix	Østgaard/Bertsch G matrix		Observed (Wheatley)	
L	F^s	F^a	F^s	F^a	F^s	F^a
0	−7.8	−3.7	−2.9	−5.4	10.07	−0.67
1	2.2	−3.0	−1.8	−1.7	6.04	−0.67
2	2.3	3.3	1.64[a]	1.46[a]		
3	2.1	2.7	0.97[a]	0.80[a]		
4	(1.6)	(1.1)	0.56[a]	0.34[a]		
5	(0.8)	(0.3)	0.45[a]	0.19[a]		

[a]Includes rearrangement contributions.

and

$$\frac{\partial\epsilon}{\partial k}=\frac{\partial T}{\partial k}+\left[\frac{\partial\Sigma}{\partial k}\right]_E+\left[\frac{\partial\Sigma}{\partial E}\right]_k\frac{\partial\epsilon}{\partial k},$$

or

$$\frac{\partial\epsilon_k}{\partial k}=\frac{\partial T_k/\partial k+(\partial\Sigma/\partial k)_E}{1-(\partial\Sigma/\partial E)_k}.$$

Thus the corresponding effective mass in the present HF approximation is

$$m^*(k,E)=\frac{M^*}{M}=\frac{1-(\partial\Sigma/\partial E)_k}{1+(M/\hbar^2k)(\partial\Sigma/\partial k)_E}. \quad (46)$$

To test the importance of the $(\partial\Sigma/\partial E)_k$ we also define an $m^*(k)$ by simply omitting this term,

$$m^*(k)=\frac{1}{1+(M/\hbar^2k)(\partial\Sigma/\partial k)_E}. \quad (47)$$

The $m^*(k)$ is often denoted[37,42] as the "k mass" since it arises from the k dependence of Σ. Similarly an "E mass" is often introduced,[37,42]

$$m^*(E)\equiv\frac{m^*(k,E)}{m^*(k)}=1-\left[\frac{\partial\Sigma}{\partial E}\right]_k, \quad (48)$$

which reflects the energy dependence of Σ. The energy dependence is contained in $\Gamma^s(k,E)$ and $(\partial\Sigma/\partial E)$ was calculated as a difference;

$$\frac{\partial\Sigma(k,E)}{\partial E}=\frac{1}{\Omega}\sum_{k_2,\sigma_2}\left[\frac{\Gamma^s(k_{12},E+\Delta)-\Gamma^s(k_{12},E)}{\Delta}\right]n(k_2).$$

We discuss in detail only m^* for the GF case. We found that in the BBG case, m^* was extremely sensitive to the rearrangement term. When it was included very large $m^*(k)$ values for $k\lesssim 0.5k_F$ were obtained [because $\epsilon(k)$ is quite flat for $k\lesssim 0.5k_F$]. With rearrangement neglected, the BBG was similar to the GF case which we now discuss.

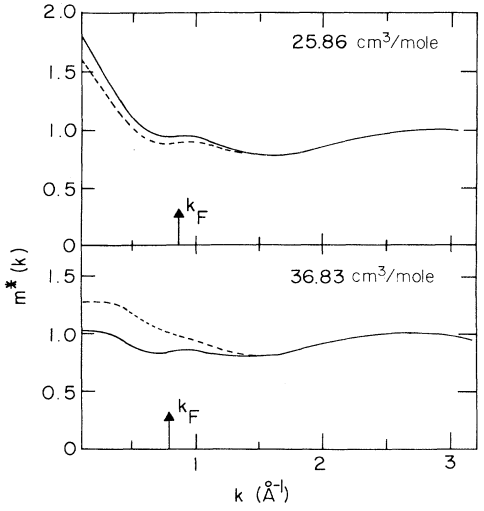

FIG. 15. "k mass" $m^*(k)$ with (solid) and without (dotted) the rearrangement term included in Σ.

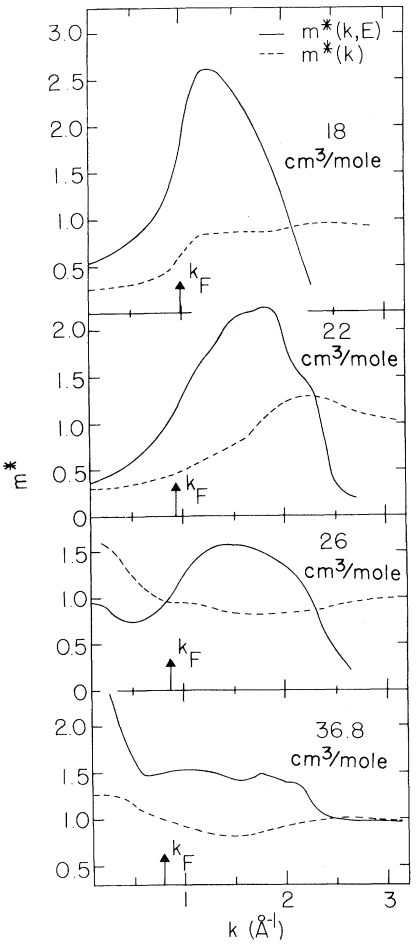

FIG. 16. "k mass" $m^*(k)$ (dotted) and the total effective mass $m^*(k,E)$ in liquid ^{3}He at four volumes calculated in the GFHF theory without rearrangement terms.

In Fig. 15 we show $m^*(k)$ in the GF case with and without the rearrangement term Σ_R of (8) included in (47). Clearly the Σ_R contributes to $m^*(k)$ for $k\lesssim 1.5k_F$ only. Its contribution is greatest at small k since from (32) $\Sigma_R(k)$ is itself largest at small k. The Σ_R contribution is always small and changes sign (as does Σ_R) when we go from a volume of 36.83 to 25.86 cm^3/mole. These volumes correspond to SVP and $p=30$ atm in real liquid ^{3}He. From here on we neglect Σ_R.

In Fig. 16 the full $m^*(k,E)$ and $m^*(k)$ at four volumes are displayed. Since the GFHF model predicts saturation at a volume $\sim$25 cm^3/mole, the $m^*(k,E)$ at $\sim$22 cm^3/mole probably best represents real liquid ^{3}He. As in Fig. 15 the $m^*(k)$ shows no strong, systematic variation with k or with volume. It varies generally between $0.3\lesssim m^*(k)\lesssim 1.3$ and, if anything, decreases as the volume is decreased. In contrast, $m^*(k,E)$ shows a strong increase or enhancement in the region $k_F\lesssim k\lesssim 2k_F$ and this enhancement increases in magnitude and is centered nearer k_F as the volume decreases. Again the $m^*(k,E)$ at $\sim$22 cm^3/mole probably best represents liquid ^{3}He at SVP and the $m^*(k,E)$ at 18 cm^3/mole ^{3}He under pressure.

An enhancement of $m^*(k,E)$ at k_F and somewhat above k_F has been obtained generally in nuclear matter[37,42] in BHF calculations. While the present results are not precise, they show that an enhancement is expected in liquid ^{3}He and can be obtained from first principles within the GFHF theory. The enhancement also increases with pressure suggesting that the increase in the observed $m^*[m^*(k_F,E)]$ with pressure may be due to increased enhancement rather than an increase in m^* at all k.

An enhancement of m^* near k_F has been proposed in liquid ^{3}He (on the basis of nuclear matter results) by Brown *et al.*[43] and by Fantoni *et al.*[44] to explain the temperature dependence of the observed C_V. Essentially, as T increases, states away from k_F will be sampled and these states will have a lower apparent effective mass so that the average m^* falls at T increases. Krotscheck and Smith[45] also obtain an enhancement using the method of correlated basis functions. Generally, higher-order terms beyond the HF theory further increase the enhancement,[37,42] and recently Friman and Krotscheck[46] proposed a second enhancement near $2k_F$.

From Fig. 15 we may also estimate the residue of the single-particle Green function at the "quasiparticle" pole:

$$z_k=\left[1-\left(\frac{\partial\Sigma}{\partial E}\right)_k\right]^{-1}=[m^*(E)]^{-1}\,. \tag{49}$$

Clearly z_k is substantially less than unity in the present model. Strictly, the Landau parameters quoted in Table VII should be renormalized by the vertex correction $z_{k_F}^2$.

VI. DISCUSSION

A central purpose of this paper was to compare the Brueckner-Bethe-Goldstone (BBG) and Galitskii-Feynman (GF) T matrices. The GF T matrix contains an additional term, $Q_H/(D-i\eta)$, in $G_2^{\rm HF}$ which is interpreted as allowing the interacting pair to scatter to intermediate hole states. For the same input (free) SPE spectrum, the BBG and GF $\Gamma(k,P)$ are identical for $k\gtrsim 1.5k_F$ because Q_H goes to zero rapidly for $k\geq k_F$. For $k\lesssim k_F$ there is some difference but it is small (see Fig. 5). Mainly the $\mathrm{Im}\Gamma(k,P)=0$ for $k\leq k_F$ in the BG case since there are no particle states available below k_F at $T=0$ K.

An important difference between the two cases emerges when the SPE spectrum and Γ are iterated. This is almost entirely due to a large rearrangement energy, Σ_R, in the BBG case and a nearly negligible Σ_R in the GF case. The larger Σ_R leads to a higher and flatter $\epsilon(k)$ for $0\leq k\leq k_F$ in the BG case. The flat $\epsilon(k)$ leads in turn to large effective-mass values. These values become increasingly and unreasonably large when the energy dependence of the self-energy $\Sigma_1(k,E)$ is included as in (46). On the other hand, the GF case gives reasonable values of $m^*(k)$, and $m^*(k,E)$ shows a strong enhancement between k_F and $2k_F$.

It could reasonably be argued that Σ_R should not be included in the definition of $\epsilon(k)$, in which event the two cases become similar. However, using the GF T matrix Σ_R is negligible, so that the distinction between the real part of the dynamical SPE and the statistical SPE in the HF approximation disappears. We found that Σ_R remains negligible in the GF case for all volumes considered. For these reasons the GF theory is preferred and leads to more consistent results independent of definitions of $\epsilon(k)$. Also, since $Q_H\to 0$ rapidly above k_F, the hole-hole term is much easier to evaluate than the particle-state term and there is no additional difficulty in including the Q_H term. For these reasons we focus on the GF results only. In future applications Σ_R need not be included.

We emphasize that in the GF formulation the zeros in D are treated correctly. With the presence of η, the formulation includes a well-defined path around the zeros in D so that there are no "singularities" in the T matrix. In practice, we integrated around the zeros in D using the standard method of (1) identifying the point on the real k axis where the zero in D occurs, (2) expanding the integrand in $\gamma_L(x,y)$ of (18) in a Taylor series about this point, and (3) integrating $\gamma_L(x,y)$ analytically over a small region centered on the zero. This region was excluded from the range of numerical integration. In this way values of $\gamma_L(x,y)$ independent of η and the excluded region size were obtained. This method works well provided the integrand does not vary rapidly where D is zero. The integrand does vary rapidly at $k=k_F$. We were able to get consistent results easily for $k=\pm 0.5$ Å^{-1} on either side of k_F. We also tried using the representation

$$\frac{1}{D\pm i\eta}=\frac{D}{D^2+\eta^2}\mp i\frac{\eta}{D^2+\eta^2}$$

and integrating numerically over the whole range, but this proved both less accurate and more time consuming.

Because of the zeros in D, the T matrix is complex. It is for this reason that we have called it a T matrix rather than a G or K matrix.[12,47] This resulting $\epsilon(k)=T(k)+\Sigma_1(k)$ is also complex. For this reason the dynamical SPE, which is complex, is probably the most consistent input SPE to use in $\Gamma(k,P)$.

The $\Gamma(k,P)$ turns out to be quite independent of $\epsilon(k)$ provided the same $\epsilon(k)$ is used for the initial and intermediate states. This can be seen comparing the Γ obtained using free-particle (kinetic) energies (Fig. 5) with that obtained using the full SC input SPE (Fig. 8). Although the SC $\epsilon(k)$ lie $\sim$15 K below the KE at low k, this difference tends to cancel between the initial and intermediate states in D giving a similar final Γ. Also in Fig. 6 we show the values of $\epsilon(k)$ obtained during the iteration toward the SC $\epsilon(k)$. The $\epsilon_1(k)$ obtained using the free-particle Γ is quite close to the final SC $\epsilon(k)$. These points mean (1) that Γ obtained using free-particle input energies is a good approximation to the SC Γ and (2) that the $\epsilon(k)$ calculated using the free-particle Γ is a reasonable approximation to the final $\epsilon(k)$.

However, for a spectrum having a gap, $\Gamma(k,P)$ is extremely sensitive to changes in $\epsilon(k)$. Generally, in the reference spectrum method, the intermediate states are fixed at free-particle energies. Changes are made to the initial states only. These changes do not cancel in D. Rather, the changes are somewhat like investigating the "off-energy-shell" dependence of $\Gamma(k,E)$ by varying the input energy $E=\epsilon_1+\epsilon_2$, and $\Gamma(k,E)$ is very energy dependent.

A second purpose here was to compare results for a continuous $\epsilon(k)$ as dictated in the GF formulation with previous work using an $\epsilon(k)$ having a gap at $k=k_F$. Firstly, the diagonal $\Gamma^s(k)$ obtained using a continuous $\epsilon(k)$ lies

approximately a factor of 3 below that obtained by Østgaard and by Brueckner and Gammel using a gap in $\epsilon(k)$ (see Fig. 13). Since the GF $\Gamma(k)$ is insensitive to changes in the continuous $\epsilon(k)$, the shallower $\Gamma(k)$ obtained by Østgaard is due entirely to having a gap in the spectrum at $k=k_F$. As a result the total liquid energy E obtained here is a factor of 3 lower than that obtained by Østgaard and by Brueckner and Gammel.

A general conclusion is that the GF T-matrix HF theory predicts a much deeper continuous single-particle excitation spectrum and a more tightly bound fluid than G or K matrices having a gap in $\epsilon(k)$. The calculated $E=-3.73$ K at $\Omega=36.83$ cm^3/mole lies well below the observed $E=-2.5$ K. To check that these results were not due to the Beck potential, we calculated Γ^s using the recent HFDHE2 potential developed by Aziz *et al.*[34] The Γ^s for the two potentials is shown in Fig. 17, and clearly they differ little. At this stage, agreement with experiment or with variational calculations[16] is not good.

The $\epsilon(k)$ here have an imaginary part and $\mathrm{Im}\epsilon(k)$ should[30] vanish at $k=k_F$ as $(k-k_F)^2$. We did not find this numerically using the definition (7) for $\epsilon(k)$. We believe this is due to approximating Γ by its on-energy-shell value in $\Sigma_1(1)$ and if the full energy dependence of Γ in (9) had been retained, $\mathrm{Im}\Sigma_1$ would vanish as required at k_F. Possible definitions of $\epsilon(k)$ and their consequences are discussed by Jeukenne *et al.*[42]

To go beyond the present GFHF results, we note that Day[48] and Mahaux[49] have discussed the HF approximation as a second-order approximation in an (hole-line) expansion of the potential in powers of a parameter κ, called the wound or depletion parameter. Physically, interactions between the fermions deplete the real-state occupation $n(k)$ from unity for $k<k_F$. The magnitude of the depletion is a good measure of the strength of the interactions. Interpreting κ as a depletion parameter we may estimate κ here as

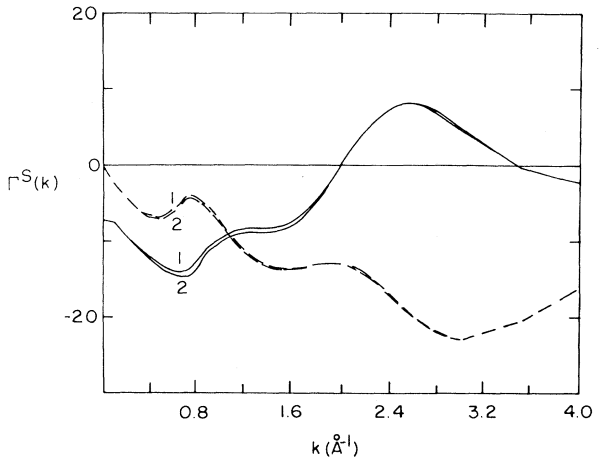

FIG. 17. GF, spin-symmetric $\Gamma^s(k)$ (diagonal and on-shell) for (1) Beck potential (Ref. 32) and (2) HFDHE2 potential (Ref. 34). —, $\mathrm{Re}\Gamma^s$; ---, $\mathrm{Im}\Gamma^s$.

$$\kappa\equiv 1-n(\langle k\rangle)=1-z(\langle k\rangle)\,,$$

where $z(k)$ is given by (49) and $\langle k\rangle$ is an average k value contributing to E (for example, $k\approx 0.75k_F$). Clearly, from Fig. 16, κ is not small, e.g., $z(\langle k\rangle)\approx 0.5$ at 36.8 cm^3/mole. Firstly, all interactions should be vertex corrected by $(1-\kappa)^2=z(k)^2$. This would certainly improve the present ground-state energy but higher-order terms would still be important. Since κ is large, we believe a better approach would be to incorporate the collective effects into Γ in a shielded potential-like approximation at the outset in an attempt to reduce Γ initially. This would be equivalent to beginning with a phononlike basis rather than a free-particle-like basis, as is done in solid helium,[50] for example. This is an approach we intend to follow

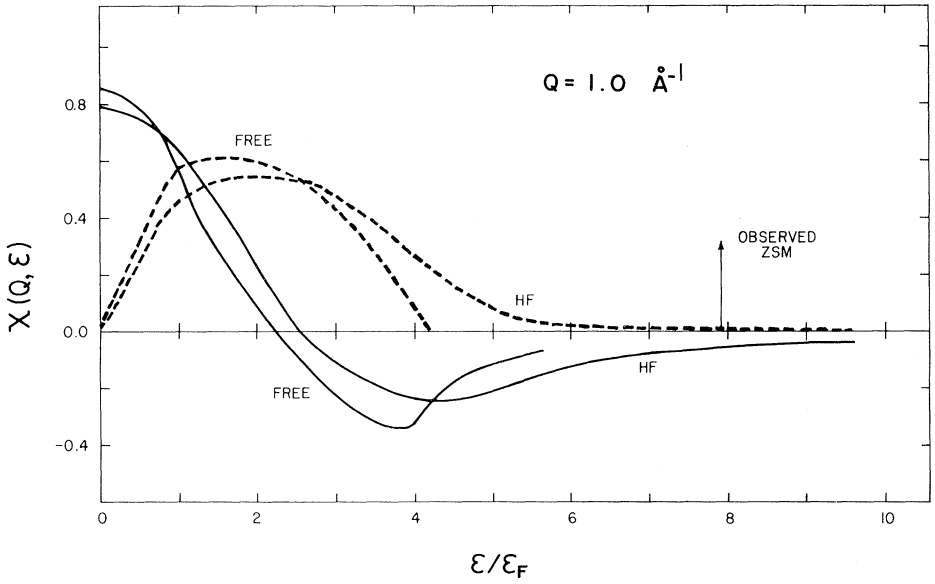

FIG. 18. Zero-order dynamic susceptibility $\chi^0(Q,\epsilon)$ [divided by $mk_F/(\pi^2\hbar^2)$] at $Q=1.0$ Å^{-1} calculated using the self-consistent Hartree-Fock energies (HF) and using free (FREE) particle energies: —, $\mathrm{Re}\chi^0$; ---, $\mathrm{Im}\chi^0$.

since calculating a series of higher-order terms does not look promising.

Also, the direct part of the Landau parameters obtained here can be used as an input to a more complete calculation. The more complete calculation must include the interaction induced via particle-hole states, not included here. For this the density-density propagator will be needed. To lowest order this is the Lindhard function,

$$\chi_0(q,\epsilon)=\frac{1}{\Omega}\sum_{k,\sigma}\frac{n(k)-n(k+q)}{\epsilon(k+q)-\epsilon(k)-(\hbar\omega+i\eta)} .$$

To illustrate the difference between the HF SC $\epsilon(k)$ and the free-particle $\epsilon(k)$, we have evaluated χ_0 using the two different $\epsilon(k)$ (Fig. 18). The HF χ_0 is spread over a somewhat larger energy range but is otherwise similar to the noninteracting χ_0. Since the direct contribution to the Landau parameters and the observed values differ so widely, an iterative approach involving Γ and χ, starting with the Γ here and χ_0, is almost certainly necessary.

Finally, the present $\Gamma(k,E)$ should represent the full effective interaction in liquid ^{3}He at high k ($k\gtrsim 2$ Å^{-1}). At high k, liquid ^{3}He does not support collective excitations[3] so that the component of the interaction induced via these excitations should disappear. The present $\Gamma(k,E)$ could therefore be used to calculate the dynamic form factor $S(q,E)$ at high $Q\gtrsim 2$ Å^{-1} for comparison with recent neutron scattering measurements.[3]

ACKNOWLEDGMENTS

It is a pleasure to acknowledge Dr. F. C. Khanna with whom this study was conceived and valuable discussions with Professor G. E. Brown, Dr. K. S. Bedell, Professor P. Nozières, and Professor C. Pethick. This work has been supported by the National Science and Engineering Research Council, Canada, and the University of Delaware.

APPENDIX

The single-particle energy in (6) is a sum of the kinetic energy, the self-energy Σ_1, and the rearrangement energy Σ_R.

1. The self-energy

To reduce Σ_1 in (7) we first sum over the spin index σ_2 ($\epsilon_1=\epsilon_1$) so that

$$\Sigma_1(1)=\frac{1}{\Omega}\sum_2[2\Gamma(12;12)-\Gamma(21;12)]n(2) . \tag{A1}$$

In relative incoming [$\vec{k}=\frac{1}{2}(\vec{k}_1-\vec{k}_2)$] and c.m. ($\vec{P}=\vec{k}_1+\vec{k}_2$) wave-vector notation this is

$$\Sigma_1(\vec{k}_1)=\frac{1}{\Omega}\sum_{(2k)}[2\Gamma(\vec{k};\vec{k},\vec{P})-\Gamma(-\vec{k};\vec{k},\vec{P})]n(2\vec{k}-\vec{k}_1) . \tag{A2}$$

Expanding Γ in partial waves as in (19), we have

$$\Gamma(\pm\vec{k};\vec{k},\vec{P})=\sum_L(2L+1)\Gamma_L(k;k,P)(\pm 1)^L , \tag{A3}$$

and from (A2)

$$\begin{aligned}\Sigma_1(\vec{k}_1)&=\frac{2}{\Omega}\sum_{(2k)}\Gamma^s(k;k,P)n(2\vec{k}-\vec{k}_1)\\&=16\int\frac{d^3k}{(2\pi)^3}\Gamma^s(k;k,P)n(2\vec{k}-\vec{k}_1) .\end{aligned} \tag{A4}$$

At $T=0$ K, this integral reduces to (24).

2. The rearrangement energy

Expressing Γ in relative coordinates and suming over the spin indices as in (A1), $\Sigma_R(k_1)$ in (8) reduces to

$$\begin{aligned}\Sigma_R(k_1)&=\frac{1}{2\Omega}\sum_{k_3,\sigma_3}\sum_{k_2}\left[\frac{\partial}{\partial n(k_1)}\Gamma^s(k;k,P)\right]n(k_2)n(k_3)\\&=\frac{1}{\Omega}\sum_{k_3,k_2}\left[\frac{\partial}{\partial n(k_1)}\Gamma^s(k;k,P)\right]n(k_2)n(k_3) .\end{aligned} \tag{A5}$$

Introducing $\Omega_0=\Omega/N$, and ignoring the dependence of Γ on P, this reduces to (Fetter and Walecka[36])

$$\Sigma_R(k_1)=\frac{2k_F^3}{\pi^2}\int_0^1 dx\,x^3\left[N\frac{\partial\Gamma^s(x;x)}{\partial n(k_1)}\right](1-\tfrac{3}{2}x+\tfrac{1}{3}x^3) , \tag{A6}$$

where $x=k/k_F$. The evaluation of the derivative in (A6) is discussed Sec. IV B.

[1]D. D. Osheroff, R. C. Richardson, and D. M. Lee, Phys. Rev. Lett. 28, 885 (1972); D. D. Osherhoff, W. J. Gully, R. C. Richardson, and D. M. Lee, *ibid.* 29, 920 (1972).

[2]For review see P. W. Anderson and W. F. Brinkman, in *The Physics of Liquid and Solid Helium, Part II,* edited by K. H. Bennemann and J. B. Ketterson (Wiley-Interscience, New York, 1978); D. M. Lee and R. C. Richardson, *ibid.;* A. J. Leggett, Rev. Mod. Phys. 47, 331 (1975); J. C. Wheatley, *ibid.* 47, 415 (1975).

[3]P. A. Hilton, R. A. Cowley, R. Scherm, and W. G. Sterling, J. Phys. C 13, L295 (1980); K. Sköld and C. A. Pelizarri, Philos. Trans. R. Soc. London Ser. B 290, 605 (1980).

[4]C. Lhuillier and F. Laloë, J. Phys. (Paris) 40, 239 (1979); 41, C7–51 (1980); B. Castaing and P. Nozières, *ibid.* 40, 257 (1979).

[5]D. S. Greywall and P. A. Busch, Phys. Rev. Lett. 49, 146 (1982).

[6]C. H. Aldrich III, C. J. Pethick, and D. Pines, Phys. Rev. Lett. 37, 845 (1976), C. H. Aldrich III and D. Pines, J. Low Temp. Phys. 32, 689 (1978).

[7]K. S. Bedell and D. Pines, Phys. Rev. Lett. 45, 39 (1980).

[8]E. Krotscheck, Phys. Rev. A 26, 3536 (1982), and references cited therein.

[9]T. L. Ainsworth, K. S. Bedell, G. E. Brown, and K. F. Quader,

J. Low Temp. Phys. 50, 317 (1983).
[10]K. Levins and O. T. Valls, Phys. Rev. B 20, 105 (1979); 20, 120 (1979).
[11]J. A. Sauls and J. W. Serene, Phys. Rev. B 24, 183 (1981).
[12]V. R. Pandharipande and R. B. Wiringa, Rev. Mod. Phys. 51, 821 (1979).
[13]L. D. Landau, Zh. Eksp. Teor. Fiz. 30, 1058 (1956) [Sov. Phys.—JETP 3, 920 (1957)]; *ibid.* 32, 59 (1957) [*ibid.* 5, 101 (1957)].
[14]For review, see G. Baym and C. Pethick, in *The Physics of Liquid and Solid Helium, Part II,* edited by K. H. Bennemann and J. B. Ketterson (Wiley-Interscience, New York, 1978).
[15]P. Nozières, *Theory of Interacting Fermi Systems* (Benjamin, New York, 1964).
[16]K. E. Schmidt, M. A. Lee, M. H. Kalos, and G. V. Chester, Phys. Rev. Lett. 47, 807 (1981); M. A. Lee, K. E. Schmidt, M. H. Kalos, and G. V. Chester, *ibid.* 46, 728 (1981); K. E. Schmidt and V. R. Pandharipande, Phys. Rev. B 19, 2504 (1979).
[17]A. A. Abrikosov and I. M. Khalatnikov, Rep. Prog. Phys. 22, 239 (1959).
[18]D. Hone, Phys. Rev. 121, 669 (1961).
[19]V. J. Emery and A. M. Sessler, Phys. Rev. 119, 43 (1960).
[20]V. J. Emery, Ann. Phys. (N.Y.) 28, 1 (1964).
[21]T. W. Burkhardt, Ann. Phys. (N.Y.) 47, 516 (1968).
[22]S. Babu and G. E. Brown, Ann. Phys. (N.Y.) 78, 1 (1973).
[23]K. A. Brueckner and J. L. Gammel, Phys. Rev. 109, 1040 (1958).
[24]K. A. Brueckner, C. A. Levinson, and H. M. Mahmond, Phys. Rev. 95, 217 (1954); K. A. Brueckner and C. A. Levinson, *ibid.* 97, 1344, (1955); K. A. Brueckner, *ibid.* 97, 1853 (1955); 100, 36 (1955).
[25]H. A. Bethe and J. Goldstone, Proc. R. Soc. London Ser. A 238, 551 (1957).
[26]E. Østgaard, (a) Phys. Rev. 187, 371 (1969); (b) 180, 263 (1969); (c) 176, 351 (1968); (d) 171, 248 (1968); (e) 170, 257 (1968).
[27]H. B. Ghassib, R. F. Bishop, and M. R. Strayer, J. Low Temp. Phys. 23, 393 (1976).
[28]R. F. Bishop, H. B. Ghassib, and M. R. Strayer, Phys. Rev. A 13, 1570 (1976).
[29]R. F. Bishop, M. R. Strayer, and J. M. Irvine, Phys. Rev. A 10, 2423 (1974); J. Low Temp. Phys. 20, 573 (1975).
[30]V. M. Galitskii and A. B. Migdal, Zh. Eksp. Teor. Fiz. 34, 139 (1958) [Sov. Phys.—JETP 7, 96 (1958)]; V. M. Galitskii, Zh. Eksp. Teor. Fiz. 34, 151 (1958) [Sov. Phys.—JETP 7, 104 (1958)].
[31]R. D. Murphy and J. A. Barker, Phys. Rev. A 3, 1037 (1971).
[32]D. E. Beck, Mol. Phys. 14, 311 (1968).
[33]J. L. Yntema and W. G. Schneider, J. Chem. Phys. 18, 646 (1950).
[34]R. A. Aziz, V. P. S. Nain, J. S. Carley, W. L. Taylor, and G. T. McConville, J. Chem. Phys. 70, 4332 (1979).
[35]P. Loubeyre, J. M. Besson, J. P. Pinceaux, and J. P. Hansen, Phys. Rev. Lett. 49, 1172 (1982).
[36]A. L. Fetter and J. D. Walecka, *Quantum Theory of Many-Particle Systems,* (McGraw-Hill, New York, 1971); see especially Chap. 4 and p. 28.
[37]A. Lejeune and C. Mahaux, Nucl. Phys. A 295, 189 (1978).
[38]B. Brandow, Rev. Mod. Phys. 39, 771 (1967).
[39]K. A. Brueckner and D. T. Goldman, Phys. Rev. 116, 1023 (1963); K. A. Brueckner, J. L. Gammel, and J. T. Kabis, *ibid.* 118, 1438 (1960).
[40]T. R. Roberts, R. H. Sherman, and S. G. Sydoriak, J. Res. Natl. Bur. Stand. 684, 567 (1964).
[41]G. F. Bertsch, Phys. Rev. 184, 187 (1969).
[42]J. P. Jeukenne, A. Lejeune, and C. Mahaux, Phys. Rep. C 25, 83 (1976).
[43]G. E. Brown, C. Pethick, and A. Zaringhalam, J. Low Temp. Phys. 48, 349 (1982).
[44]S. Fantoni, V. R. Pandharipande, and K. E. Schmidt, Phys. Rev. Lett. 48, 878 (1982).
[45]E. Krotscheck and R. A. Smith, Phys. Rev. B 27, 4222 (1983).
[46]B. L. Friman and E. Krotscheck, Phys. Rev. Lett. 49, 1705 (1982).
[47]G. E. Brown, Rev. Mod. Phys. 43, 1 (1971).
[48]B. D. Day, Rev. Mod. Phys. 50, 495 (1978).
[49]C. Mahaux, in *The Many-Body Problem, Jastrow Correlations Versus Brueckner Theory,* Vol. 138 of *Springer Lecture Notes in Physics,* edited by R. Guardiola and J. Ros (Springer, Berlin, 1980).
[50]H. R. Glyde and F. C. Khanna, Can. J. Phys. 49, 2997 (1971).